MARIA ANTONIA MACHADO BARBOSA

HOMOBARIC AND HETEROBARIC LEAVES IN TOMATO (S*olanum lycopersicum* L.): MORPHOLOGICAL, ANATOMICAL AND PHYSIOLOGICAL IMPLICATIONS IN DIFFERENT ENVIRONMENTAL CONDITIONS

Dissertation submitted to Federal University of Viçosa, as part of the requirements for obtaining the *Magister Scientiae* degree in Plant Physiology.

VIÇOSA
MINAS GERAIS – BRAZIL
2017

Ficha catalográfica preparada pela Biblioteca Central da Universidade Federal de Viçosa - Câmpus Viçosa

T
B238h
2017

Barbosa, Maria Antonia Machado, 1984-
Homobaric and heterobaric leaves in tomato (*Solanum lycopersicum* L.) : morphological, anatomical and physiological implications in different environmental conditions / Maria Antonia Machado Barbosa. – Viçosa, MG, 2017.
vii, 85f. : il. (algumas color.) ; 29 cm.

Orientador: Agustin Zsögön.
Dissertação (mestrado) - Universidade Federal de Viçosa.
Inclui bibliografia.

1. Tomate. 2. *Solanum lycopersicum*. 3. Folhas - Anatomia. 4. Análise foliar. 5. Folhas - Aspectos ambientais. I. Universidade Federal de Viçosa. Departamento de Biologia Vegetal. Programa de Pós-graduação em Fisiologia Vegetal. II. Título.

CDD 22 ed. 635.642

MARIA ANTONIA MACHADO BARBOSA

HOMOBARIC AND HETEROBARIC LEAVES IN TOMATO (*Solanum lycopersicum* L.): MORPHOLOGICAL, ANATOMICAL AND PHYSIOLOGICAL IMPLICATIONS IN DIFFERENT ENVIRONMENTAL CONDITIONS

Dissertation submitted to Federal University of Viçosa, as part of the requirements for obtaining the *Magister Scientiae* degree in Plant Physiology.

APPROVED: July 17th, 2017

Adriano Nunes Nesi

Samuel Cordeiro Vitor Martins

Dimas Mendes Ribeiro

(Co-adviser)

Agustin Zsögön

(Adviser)

I offer

to my dear family. My parents Antonio José and Maria Lúcia, my sisters Marilane, Aldiane and Eliane and my brother Erlan. To my dear and affectionate auntie Liduina Eloi (in memoriam).

"I am always in front of you, behind you, and also by your side, guiding you every day (...). I have a perfect and beautiful plan and it is for your good. Even before his body formed, I had planned all his days."

Salm 139

ACKNOWLEDGEMENTS

Primarily, my thanks are directed to God, for being my peace, strength and help in the face of difficulties.

Thank you to my family for unconditional support and understanding.

Thanks the Universidade Federal de Viçosa, especially the Plant Physiology Graduate Program, for infrastructure and ease during the development of this work. Thanks are also to Capes, which has provided me a scholarship in the last two years.

I am very thankful to Prof Dr. Agustin Zsögön for his teachings, guidance and confidence directed to me for the development of this project.

To the Prof Dr. Dimas Ribeiro for the supervision, collaboration and for his excellent suggestions during the development of this research, my thank you!

My thanks are also to Prof Dra. Aristéa Azevedo for the attention and transfer of her knowledge in plant anatomy, as well as her life experiences. To Prof Dr. Samuel Cordeiro Martins (Samuca) for his unparalleled ability to pass on his knowledge and his great readiness to collaborate with this project.

For my friends Odyone Nascimento and Gélia Viana, for the friendship, companionship and help, besides representing my family during these two years in Viçosa.

To friends of the Laboratory of Molecular Plant Physiology: Jessenia Moncaleano, Julienne Moreira, Emmanuel Naves, João Vitor, Carla Bastos, Giuliana Mourão, Túlio Pacheco, Amanda Lopes, Karla Gasparini and Fernanda Sartor, for the experiences, companionship and good laughs, thank you!

Last, but not least, thanks to all colleagues who contributed to this work and were not nominated. My sincerest thanks!

CONTENTS

ABSTRACT

BARBOSA, Maria Antonia Machado, M.Sc., Universidade Federal of Viçosa, July, 2017. **Homobaric and hererobaric leaves in tomato (*Solanum lycopersicum* L.): morphological, anatomical and physiological implications in different environmental conditions.** Adviser: Agustin Zsögön; Co-adviser: Dimas Mendes Ribeiro.

Homobaric and heterobaric leaves are characterized, respectively, by the absence and presence of bundle sheath extensions (BSEs), a structure formed by parenchymatic cells which connects the leaf epidermis to the vascular bundles. Species that have heterobaric leaves present less resistance to water transport, however, homobaric leaves are less hydraulically integrated and have greater resistance to water movement. The objective of this work was to evaluate the influence of BSE on tomato plants under different environmental conditions. This dissertation was divided into two chapters: 1- an evaluation of the structure and physiology of homobaric and heterobaric plants grown in different irradiance conditions and 2- response to soil water deficit. We have shown that the presence of BSE altered the coordination between lamina thickness and structural and biochemical parameters in response to different levels of irradiance. Heterobaric leaves showed phenotypic plasticity, mainly in relation to vein density and SPI, showing that BSE acts by coordinating the flow of water from the vascular bundle to the epidermis, when the levels of irradiance are low. The homobaric mutant, whose BSE is absent, showed a response pattern, whereby the plastic response is transferred to a different set of characteristics that were not affected in heterobaric plants. Also, the plants that harbor the *obv* mutation exhibited a reduced leaf rolling, higher values of TRA and leaf water potential in comparison with heterobaric leaves, in the condition of water deficit, suggesting that the absence of BSE positively influenced the response of these plants in dry condition. Lastly, we present our conclusions in a final section, where we discuss how this work could contribute to increased understanding of the relationship between form and function in angiosperm leaves.

RESUMO

BARBOSA, Maria Antonia Machado, M.Sc., Universidade Federal de Viçosa, julho de 2017. **Folhas homobáricas e heterobáricas em tomateiro (*Solanum lycopersicum* L.): implicações morfológicas, anatômicas e fisiológicas em diferentes condições ambientais.** Orientador: Agustin Zsögön. Coorientador: Dimas Mendes Ribeiro.

Folhas homobáricas e heterobáricas são caracterizadas, respectivamente, pela ausência e presença da extensão da bainha do feixe (BSE), uma estrutura formada por células parenquimáticas que conectam a epiderme foliar aos feixes vasculares. Espécies que possuem folhas heterobáricas apresentam menor resistência ao transporte de água, no entanto, folhas homobáricas são menos hidraulicamente integradas e têm maior resistência ao movimento da água. Esse trabalho teve como objetivo, avaliar a influência da BSE em plantas de tomate sob diferentes condições ambientais. Esta dissertação foi dividida em dois capítulos: 1- uma avaliação da estrutura e fisiologia das plantas homobáricas e heterobáricas cultivadas em diferentes condições de irradiância e 2- sua resposta ao déficit hídrico do solo. Nós mostramos que a presença de BSE alterou a coordenação entre espessura da lamina e parâmetros estruturais e bioquímicos em resposta a diferentes níveis de irradiancia. Folhas heterobáricas apresentaram plasticidade fenotípica, principalmente em relação à densidade da venação e SPI, mostrando que a BSE atua coordenando o fluxo de água do feixe vascular para a epiderme, quando os níveis de irradiação são baixos. O mutante homobárico, cuja BSE é ausente, mostrou um padrão de resposta, através do qual, a resposta plástica é transferida para um conjunto diferente características que não foram afetadas em plantas heterobáricas. E ainda, as plantas que abrigam a mutação *obv*, exibiram um reduzido enrolamento das folhas, maiores valores de TRA e potencial hídrico foliar em comparação com folhas heterobáricas, em condição de déficit hídrico, sugerindo que a ausência de BSE influenciou positivamente a resposta dessas plantas em condição de seca. Por fim, apresentamos nossas conclusões em uma seção final, onde discutimos como esse trabalho poderia contribuir para uma maior compreensão da relação entre a forma e a função nas folhas de angiosperma.

GENERAL INTRODUCTION

The flow of water encounters resistance throughout the body of the plant, the leaf being the organ where the largest portion of the resistance is found (SACK & HOLBROOK, 2006b). When leaving the xylem, water passes through multiple cells in the extra-vascular space, where the foliar hydraulic conductivity becomes dependent on the leaf anatomy, which is substantially variable between species (LYNCH et al., 2012; TAIZ & ZEIGER, 2013).

The leaves often face imbalances in transpiration rates, in response to variations in stomatal opening which, among other factors, is also associated with the internal hydraulic environment of leaves (PRADO & MAUREL, 2013). The veins act as mechanical support for the leaves, and favor the entrance of light and transport of photo-assimilates to the body of the plant.

At the end of the 19th century, german anatomists described the presence of structures formed by parenchyma cells, which interconnect the leaf epidermis to the ribs, being able to be bound in both the adaxial and abaxial epidermis, or both, in leaves of angiosperms, being then called "bundle sheath extension" (BSEs) (WYLIE, 1943; WYLIE, 1952). BSEs are presented as compact and pigment-free cells that give rise to a network of clear veins on a dark green leaf blade due to the absence of the parenchymal cell column connecting the vascular bundle to the epidermis and the presence of cells containing chlorophylls (WYLIE, 1952; MCCLENDON, 1992; KARABOURNIOTIS et al., 2000).

The presence or absence of BSEs in the epidermis classifies the leaves as heterobaric and homobaric, respectively, and these structures may be associated with hydraulic functions in leaves (TERASHIMA, 1992b; BRODRIBB et al., 2007). Species that have heterobaric leaves, present less resistance for the transport of water (BUCKLEY; SACK; GILBERT, 2011). In contrast, homobaric leaves are less hydraulically integrated and have a higher resistance to water movement (ZWIENIECKI et al., 2007). In addition, it is known that BSEs occur more frequently in leaves of tropical forest tree species, as well as herbaceous canopy

plants, which are under conditions of high solar irradiance and high temperature (KENZO et al., 2007). The higher frequency of trees with heterobarics leaves suggests that the presence of BSEs confer an advantage to canopy plants. In the sub-forest, the highest proportion of species with homobaric leaves is an indication that the absence of BSEs can improve the ability of these plants to use occasional small flashes of light (PIERUSCHKA et al., 2006).

Environmental changes may promote phenotypic changes in plants at morphological and physiological levels that may be crucial for the survival of individuals (GRATANI, 2014). When the plants are exposed to different light intensities, changes in internode length, petiole, changes in leaf shape and size, among others (SCHULTZ & MATTHEWS, 1993; CHITWOOD et al., 2015). In addition, in a situation of low soil water supply, the great diversity of leaves with their variable characteristics may also be directly related to the survival of the plants under these conditions, because the leaves are the final components of the transpiration flow and their hydraulic properties significantly affect the hydraulic conductance of the whole plant (K_{plant}) (SACK et al., 2003).

In tomato (*Solanum lycopersicum* L.), the leaves are classified as heterobaric (THOMPSON et al., 2007). However, Jones et al. (2007) observed in commercial tomatoes that some varieties had veins of coloration as dark as internerval areas, due to the recessive mutation called *obscuravenosa* (*obv*). Zsögön et al. (2015) reassessed the description of the mutant, establishing that they are leaves that lack BSEs completely developed, and therefore are homobaric. They proposed to evaluate the differences between homobaric and heterobaric leaves by creating isogenic *obv* strains, where the *obv* mutation of the cultivar M82 (a commercial cultivar) was introduced into the Micro-Tom cultivar by means of successive backcrosses to allow comparative studies in the same genetic *background* (CARVALHO et al., 2011; STAM & ZEVEN, 1981), since the studies related to the effect of homobaric and heterobaric leaves on the efficiency of the plants until then were based on comparisons made in different species, such as tree species (INOUE et al., 2015).

Studies on the development and function of leaf veins have been of increasing interest, as they are directly associated with the performance of plants, both agronomically and ecologically (SACK et al., 2012). Thus, it is of great importance to investigate the influence of leaf structures under influence of environmental changes.

GENERAL OBJECTIVES

To investigate the influence of homobaric and heterobaric leaves on the physiological responses of tomato under different environmental conditions, such as different levels of irradiance and water supply.

SPECIFIC OBJECTIVES

1. To determine the effect of different irradiance levels on the hydraulic conductance (K_{leaf}) of tomato leaves with and without BSEs;
2. To evaluate the influence of sun and shade treatments on the form and structure of homobaric and heterobaric leaves in tomato;
3. To compare gas exchange and chlorophyll fluorescence in homobaric and heterobaric leaves of tomato under two levels of irradiance;
4. To analyze the gas exchange and the water status of tomato plants with homobaric and heterobaric leaves under conditions of water deficit;
5. To evaluate the effects of water deficit in leaf foliage on homobaric and heterobaric tomatoes;
6. Observe stomatal dynamics in homobaric and heterobaric leaves of tomato in response to leaf irradiance and excision;
7. Investigate the effects of exogenous application of abscisic acid (ABA) and under the stomatal closure of leaves with and without BSEs in tomato;

LITERATURE CITED

Brodribb TJ, Feild TS, Jordan GJ (2007) Leaf maximum photosynthetic rate and venation are linked by hydraulics. Plant Physiol **144**: 1890–1898

Buckley TN, Sack L, Gilbert ME (2011) The role of bundle sheath extensions and life form in stomatal responses to leaf water status. Plant Physiol **156**: 962–973

Carvalho RF, Campos ML, Pino LE, Crestana SL, Zsögön A, Lima JE, Benedito VA, Peres LE (2011) Convergence of developmental mutants into a single tomato model system: "Micro-Tom" as an effective toolkit for plant development research. Plant Methods **7**: 18

Chitwood DH, Kumar R, Ranjan A, Pelletier JM, Townsley BT, Ichihashi Y, Martinez CC, Zumstein K, Harada JJ, Maloof JN, e outros (2015) Light-induced indeterminacy alters shade-avoiding tomato leaf morphology. Plant Physiol **169**: 2030–2047

Gratani L (2014) Plant phenotypic plasticity in response to environmental factors. Adv Bot **2014**: 1–17

Inoue Y, Kenzo T, Yoneyama A, Ichie T (2015) Leaf water use in heterobaric and homobaric leafed canopy tree species in a Malaysian tropical rain forest. Photosynth **53**: 177–186

Jones CM, Rick CM, Adams D, Jernstedt J, Chetelat RT (2007) Genealogy and fine mapping of *obscuravenosa*, a gene affecting the distribution of chloroplasts in leaf veins, and evidence of selection during breeding of tomatoes (*Lycopersicon esculentum*; Solanaceae). Am J Bot **94**: 935–947

Karabourniotis G, Bornman JF, Nikolopoulos D (2000) A possible optical role of the bundle sheath extensions of the heterobaric leaves of *Vitis vinifera* and *Quercus coccifera*. Plant, Cell Environ **23**: 423–430

Kenzo T, Ichie T, Watanabe Y, Hiromi T (2007) Ecological distribution of homobaric and heterobaric leaves in tree species os Malaysian lowland tropical rainforest. Am J Bot **94**: 764-775

Lynch DJ, McINerney FA, Kouwenberg LLR, Gonzalez-Meler MA (2012) Plasticity in bundle sheath extensions of heterobaric leaves Am J Bot **99**: 1197–1206

McClendon JH (1992) Photographic survey of the occurrence of bundle-sheath extensions in deciduous dicots. Plant Physiol **99**: 1677–1679

Pieruschka R, Schurr U, Jensen M, Wolff WF, Jahnke S (2006) Lateral diffusion of CO_2 from shaded to illuminated leaf parts affects photosynthesis inside homobaric leaves. New Phytol **169**: 779–788

Prado K, Maurel C (2013) Regulation of leaf hydraulics: from molecular to whole plant levels. Front Plant Sci **4**: 1–14

Sack L, Cowan PD, Jaikumar N, Holbrook NM (2003) The "hydrology" of leaves: co ordination of structure and function in temperate woody species. Plant, Cell Environ **26**: 1343–1356

Sack L, Holbrook NM (2006) Leaf hydraulics. Annu Rev Plant Biol **57**: 361-381

Sack L, Scoffoni C, McKown AD, Frole K, Rawls M, Havran JC, Tran H, Tran T (2012) Developmentally based scaling of leaf venation architecture explains global ecological patterns. Nat Commun **3**: 837

Schultz HR, Matthews MA (1993) Xylem development and hydraulic conductance in sun and shade shoots of grapevine (*Vitis vinifera* L.): evidence that low light cuncouples water transport capacity from leaf area. Planta **190**: 393–406

Stam P, Zeven AC (1981) The theoretical proportion of the donor genome in near-isogenic lines of self-fertilizers bred by backcrossing. Euphytica **30**: 227–238

Taiz L, Zeiger E (2013) Plant Physiology - Taiz & Zeiger - 5ª edition. 782

Terashima I (1992) Anatomy of non-uniform leaf photosynthesis. Photosynth Res **31**: 195–212

Thompson AJ, Andrews J, Mulholland BJ, Mckee JMT, Hilton HW, Horridge JS, Farquhar GD, Smeeton RC, Smillie IRA, Black CR, e outros (2007) Overproduction of abscisic acid in tomato increases transpiration eficiency and root hydraulic conductivity and in uences leaf expansion. Plant Physiol **143**: 1905–1917

Wylie RB (1952) The bundle sheath extension in leaves of dicotyledons. Am J Bot **39**: 645–651

Wylie RB (1943) The role of the epidermis in foliar organization and its relations to the minor venation. Am J Bot **30**: 273–280

Zsögön A, Peres P, Nguyen HT, Ball MC (2015) A mutation that eliminates bundle sheath extensions reduces leaf hydraulic conductance , stomatal conductance and assimilation rates in tomato (*Solanum lycopersicum*). New Phytol **205**: 618-626

Zwieniecki MA, Brodribb TJ, Holbrook NM (2007) Hydraulic design of leaves : insights from rehydration kinetics. Plant, Cell Environ **30**: 910–921

CHAPTER I

Bundle sheath extensions affect leaf phenotypic plasticity in response to irradiance in tomato

Authors: Maria Antonia M. Barbosa[1], Daniel H. Chitwood[2]; Aristea A. Azevedo[1]; Lázaro E. P. Peres[3]; Wagner L. Araújo[1,4]; Samuel Cordeiro Vitor Martins[1]; Dimas Mendes Ribeiro[1]; Agustin Zsögön[1*]

Affiliations

[1]*Departamento de Biologia Vegetal, Universidade Federal de Viçosa, CEP 36570-900, Viçosa, MG, Brazil*

[2]*Independent Researcher, Santa Rosa, CA 95409 USA*

[3]*Laboratory of Hormonal Control of Plant Development. Departamento de Ciências Biológicas, Escola Superior de Agricultura "Luiz de Queiroz", Universidade de São Paulo, CP 09, 13418-900, Piracicaba, SP, Brazil*

[4]*Max-Planck Partner group at the Departamento de Biologia Vegetal, Universidade Federal de Viçosa, 36570-900, Viçosa, MG, Brazil.*

Key words: leaf structure, morphogenesis, hydraulic conductance, shading, *obscuravenosa*, *Solanum lycopersicum*

Abstract

Coordination between structural and physiological traits is key to plants responses to environmental fluctuations. This is especially relevant to leaf hydraulics, as plant face constant imbalances between water supply and demand. Heterobaric leaves present an efficient transport of water to the epidermis, due to the presence of bundle sheath extensions (BSEs), which increase the capacity for water transport, measured as leaf hydraulic conductance (K_{leaf}). On the other hand, homobaric leaves are less hydraulically integrated and have a higher resistance to water movement. Tomato leaves (*Solanum lycopersicum* L.) are classified as heterobaric, however, the

obscuravenosa (*obv*) mutation, which is found in many commercial tomato varieties, lacks BSEs. We examined structural and physiological traits in plants grown at different irradiance levels (sun/shade, 900/300 μmol photons m^{-2} s^{-1}) for heterobaric (MT) and homobaric (*obv*) leaves of tomato plants. We show that K_{leaf} varies in proportion to irradiance in heterobaric leaves but not in homobaric leaves, where K_{leaf} values are kept low in both environments. This result is in line with a similar pattern of variation for leaf shape and area, stomatal and vein density and stomatal conductance. Photosynthetic assimilation rate, however, is maintained high in shade homobaric plants along with increased chlorophyll and soluble protein contents and greater intercellular air spaces in the leaf. The result is that leaf and whole plant dry mass, as well as tomato yield, were altered by irradiance level but not by genotype. We propose that BSEs confer plasticity in traits related to leaf structure and function in response to light intensity, but that their absence can be compensated by a plastic response on a different set of traits, thus producing a similar phenotypic result in terms of carbon economy and plant productivity.

Introduction

The plethora of structural variation found in leaves has been interpreted either as close developmental tracking of environmental conditions or a relatively loose connection between form and function, which has allowed for high plasticity provided a minimal level of performance is maintained (Niklas, 1992). The coordination of leaf structure with hydraulic design is of paramount importance for plant function, acclimation to the environment and ecological distribution (Nicotra et al., 2008; Nicotra et al., 2011). The rate of water transport through the leaf is a fine balancing act dictated by resource supply and demand dynamics and constrained by the laws of biophysics (Brodribb, 2009; Buckley et al., 2016).

Water flow through the plant body is analogous to an electric circuit, with a series of additive resistances between the soil and the atmosphere (Sack e Holbrook, 2006). In this system, the leaf constitutes a hydraulic bottleneck and a strong

determinant of whole-plant performance. This is due to the large contribution of stomata to leaf hydraulic resistance (R_{leaf}). R_{leaf} is dynamic and can vary with time of day, irradiance, temperature and water availability. The efficiency of water transport through the leaf is measured as K_{leaf} (leaf hydraulic conductance, $R_{leaf}=1/K_{leaf}$). Other leaf architectural traits have been dissected and are also well-known to reciprocally influence K_{leaf} (*e.g.* leaf thickness, stomatal pore area, chlorophyll concentration, lamina margin dissection, among others).

In particular, venation structure and patterning play a critical role in water distribution (Sack et al., 2012; Sack e Scoffoni, 2013). Water flow through the leaf occurs through xylem conduits within the vascular bundles, which upon entering the lamina from the petiole rearrange into major and minor veins. The midrib (primary), secondary and tertiary veins are involved mainly in water supply, whereas higher order veins (quaternary, and so on) are involved in water distribution throughout the lamina. Hydrated leaves with higher K_{leaf} (K^{max}_{leaf}) usually have greater midrib caliber, and higher minor vein density. Water movement outside the xylem is more difficult to study and quantify, but the extra-xylematic pathway probably contributes at least as much to R_{leaf} as the xylem pathways. It is still not clear whether this flow occurs through symplastic, apoplastic pathways, or a combination of both (Buckley et al., 2015).

Upon leaving the xylem, water has to transit through the bundle sheath, a layer of compactly arranged parenchymatic cells surrounding the vasculature. (Esau, 1977). Bundle sheaths could behave as flux sensors or 'control centers' of leaf water transport, and are possibly responsible for the high dependence of K_{leaf} on temperature and irradiance (Sack e Holbrook, 2006a; Leegood, 2008). Vertical layers of colorless cells connecting the vascular bundle to the epidermis are present in many eudicotyledons. These so-called bundle sheath extensions (BSEs) are most commonly found in minor veins, but can occur in veins of any order depending on the species (Wylie, 1952). A topological consequence of the presence of BSEs is the formation of compartments in the lamina, which restricts lateral gas flow and thus

allows compartments to maintain gas exchange rates independent of one another. Such leaves, and by extension the species possessing them, are therefore called ‘heterobaric’, as opposed to ‘homobaric’ species lacking BSEs.

Large taxonomical surveys showed that heterobaric species tend to occur more frequently in sunny and dry sites or in the upper stories of climax forests (Kenzo et al., 2007), so it was hypothesized that BSEs could fulfill an ecological role by affecting mechanical and physiological parameters in the leaf (Terashima, 1992a). Some of these functions, such as providing mechanical support (Read e Stokes, 2006), protecting the leaf from mechanical damage or restricting the spread of disease (Lawson e Morison, 2006), remain hypothetical. Other functions, however, have been proven through meticulous experimental work, suggesting that the existence of BSEs could be adaptive (Buckley et al., 2011). Lateral propagation of ice in the lamina was precluded by the sclerenchymatic BSEs in *Cinnamomum canphora* L (Hacker e Neuner, 2007). Hydraulic integration of the lamina is increased by BSEs, which connect the vascular bundle to the epidermis and therefore shorten the water path between the supply structures (veins) and the water vapor outlets (stomata) (Zwieniecki et al., 2007). Photosynthetic assimilation rates are increased in leaves with BSEs, due to their optimization of light transmission within the leaf blade (Karabourniotis et al., 2000; Nikolopoulos et al., 2002).

Most of the above studies addressing the function of BSEs are generally based on large-scale multi-species comparisons, which restricts the conclusions to a statistical effect. Many structural and hydraulic leaf traits are strongly co-ordinated and co-selected, therefore reducing the discriminating power of analyses involving species of different life forms and ecological background. We have previously characterized a mutant that lacks BSEs in the otherwise heterobaric species tomato (*Solanum lycopersicum* L.) (Zsögön et al., 2015). The homobaric mutant *obscuravenosa* (*obv*) reduces K_{leaf} and stomatal conductance but does not impact global carbon economy of the plants. Here, we extend our observations to plants grown under two contrasting irradiance levels, which are known to influence both

leaf structure (Oguchi et al., 2003; Oguchi et al., 2005; Oguchi et al., 2006) and K_{leaf} (Scoffoni *et al.*, 2008; Guyot *et al.*, 2012). We tested whether the presence of BSEs could have an impact on the highly plastic nature of leaf development and function in response to different irradiance levels. We cultivated plants of tomato and the *obv* mutant in two irradiance levels and assessed a series of structural parameters such as leaf area, shape, vein and stomatal density, as well as physiological ones, among them, K_{leaf}, assimilation rate, stomatal conductance and photosystem II efficiency. Finally, we analysed whether dry mass accumulation and tomato fruit yield. We discuss the potential role of BSEs in the coordination of hydraulics with leaf structure in response to the light environment.

Materials and Methods

Plant material

Seeds of the tomato (*Solanum lycopersicum* L.) cv Micro-Tom (MT) and cv M82 were kindly donated by Dr Avram Levy (Weizmann Institute of Science, Israel) and Dr Roger Chetelat (Tomato Genetics Resource Center, Davis, University of California, CA, USA), respectively. The introgression of the *obscuravenosa* (*obv*) into the MT genetic background was described previously (Carvalho et al., 2011). The tomato M82 cultivar harbors the *obv* mutation, so the experiments were performed on F1 lines obtained by crosses between MT and M82 (Figure S1; described in Table 1).

Table 1. Description of the plant material used in this study. Micro-Tom (MT) and M82 are two tomato cultivars that differ in growth habit due mostly (but not only, see (Campos et al., 2010) for details) to the presence of a mutant allele of the *DWARF* gene (functional allele capitalized), a brassinosteroid C-6 oxidase, whose product is required for a fully functional brassinosteroid biosynthesis pathway. The molecular identity of *OBSCURAVENOSA* (*OBV*) is unknown. MT harbors a functional, dominant allele of *OBV*, whereas M82 is a mutant, as shown by (Jones et al., 2007). F1 plants are hybrids with a 50/50 MT/M82 genomic complement, differing only in the presence or absence of BSEs. The F1 plants are otherwise phenotypically indistinguishable from the M82 parent. For simplicity, the F1 lines with and without BSEs are referred to as M82 and *obv*.

Parental genotype	MT	MT-*obv*	M82	MT×M82	MT-*obv*×M82
Growth habit					
Genotype	*dwarf/dwarf*	*dwarf/dwarf*	*DWARF/DWARF*	*DWARF/dwarf*	*DWARF/dwarf*
Phenotype	Dwarf plant	Dwarf plant	Tall plant	Tall plant	Tall plant
BSE					
Genotype	*OBV/OBV*	*obv/obv*	*obv/obv*	*OBV/obv*	*obv/obv*
Phenotype	BSEs (clear veins)	No BSEs (dark veins)	No BSEs (dark veins)	BSEs (clear veins)	No BSEs (dark veins)

Growth conditions

Data were obtained from two independent assays. Plants were grown in a greenhouse in Viçosa (642 m asl, 20º 45' S; 42º 51' W), Minas Gerais, Brazil, under semi-controlled conditions. Micro-Tom (MT) background plants were grown during the months of May to August of 2016 in temperature of 23/19°C, 11/13h (day/night) photoperiod and relative humidity of 85/75%. Plants in the M82 background were cultivated during the months of September to December of 2016 with temperatures of 26/21°C, 12/12h (day/night) photoperiod and relative humidity of 65/80%. Seeds were germinated in polyethylene trays with commercial substrate Tropostrato® (Vida Verde, Mogi Mirim, SP, Brazil) and supplemented with 1g L^{-1} 10:10:10 NPK and 4 g L^{-1} dolomite limestone ($MgCO_3$ + $CaCO_3$). Weekly foliar fertilization was carried out using 2 g L^{-1} Biofert® leaf fertilizer 6-4-14 (Biokits, Contagem, MG,

Brazil). Upon appearance of the first true leaf, seedlings of each genotype were transplanted to pots with a capacity of 0.3L and 3.5L for MT and M82, respectively. The new pots were filled with substrate as described above, except for the NPK supplementation, which was increased to 8 g L^{-1}. Irrigation was performed daily, twice a day, in a controlled manner, so that each vessel received the same volume of water.

Experimental setup

The two experiments were conducted in completely randomized experimental design, in 2×2 factorial, consisting of two genotypes, and two irradiance levels (sun and shade). Plants in the 'sun' treatment were exposed to greenhouse conditions, with midday irradiance of ~900 μmol photons m^{-2} s^{-1}. For the 'shade' treatment plants were maintained on a separate bench covered with neutral shade cloth, with a retention capacity of 70% of sunlight (250-300 μmol photons m^{-2} s^{-1}).

Plant morphology determinations

Morphological characterization was performed in MT plants 50 days after germination (plants presented a consistent delay in growth, due to the low temperature in the initial period of the experiment). The height of the plants was taken from the measurement of the plant from the ground level to the upper apical node. The number of leaves to the first inflorescence was obtained by counting the number of leaves on the main stem, from the bottom up. The foliar angle were determined with the aid of a protractor, based on the insertion of the 5^{th} leaf. Stem diameter was measured using a mechanical pachymeter (Mitutoyo® Vernie Caliper model, Japan) and measurements were made at the base of the plant. All these morphological parameters were evaluated in eight plants per treatment. Total leaf area and specific leaf area (SLA) were evaluated in five plants per treatment. The

total leaf area was calculated digitizing all leaves with an HP Scanjet G2410 scanner (Hewlett-Packard, Palo Alto, California, USA), and then calculating the area using ImageJ® (http://rsbweb.nih.gov/ij/). The determination of SLA was carried out in fully expanded fourth leaf was taken as the base that was collected and digitized (HP Scanjet G2410 scanner, Hewlett-Packard, Palo Alto, California, USA), being obtained its area and later dry mass in oven at 70ºC for 72h. SLA was calculated through the relationship between leaf area (LA) and dry mass (LDW), as described by the equation:

$$SLA\ (cm^2\ g^{-1}) = LA/LDW$$

Branching pattern was carried out in six replicates and assessed through visual observation and scoring three types of ramification stages in the leaf axils: no primordium, visible primordium and fully-developed branch. Plant growth evaluation was determined from root, stem and leaves dry mass data by destructive analysis 65 days after germination, in five plants per treatment. Root, stem and leaf were collected separately and packed in paper bags and oven dried at 70°C for 72h until they reached constant weight. The samples were then weighed in a semi-analytical balance (AUY220, Shimadzu, Kyoto, Japan) with a sensitivity of 0.01 g.

Elliptical Fourier Descriptor analysis of leaflet shape

Leaflets were dissected from leaves of MT and *obv* plants grown under sun and shade conditions and scanned on a white background. From each leaf, the terminal leaflet and the two most distal leaflet pairs of fourth fully expanded, were isolated using binary thresholding functions in ImageJ® software (http://rsbweb.nih.gov/ij/) (Abramoff et al., 2004) and converted to .bmp files for analysis in SHAPE (Iwata e Ukai, 2002), where each leaflet was converted into chaincode, oriented, and decomposed into harmonic coefficients. The harmonic coefficients were then converted into a data frame format and read into R (R Core Team, 2017). The Momocs package (Bonhomme et al., 2014) was used to visualize

mean leaflet shapes from each genotype/light treatment combination. The prcomp() function was used to perform a Principal Component Analysis (PCA) on only A and D harmonics so that only symmetric (rather than asymmetric) shape variance was considered (Iwata et al., 1998). The results visualized using ggplot2 (Wickham, 2016).

Microscopy analyses

All anatomical analyses were performed in plants 50 days after germination in six replicates per treatment. Epidermal and leaf blade traits were determined in MT and MT-*obv*. For vein density, epidermal pavement cell size, stomatal density, guard cells size, and stomatal index on the adaxial and abaxial faces, the fully expanded fifth leaf was used, cleared with 95% methanol for 48h followed by 100% lactic acid. Images obtained in a light microscope (Zeiss, Axioscope A1 model, Thornwood, NY, USA) with attached Axiovision® 105 color image capture system, were evaluated in the Image Pro-Plus® software (version 4.5, Media Cybernetics, Silver Spring, USA). Areas of 7.9 mm^2 Stomatal density was calculated as number of stomata per unit leaf area, stomatal index as the proportion of guard cells to total epidermal cells. Minor vein density was measured in area of 15 mm^2 as length of minor veins (<0.05 µm caliber) per unit leaf area.

For cross-sectional analyses, samples were collected from the medial region of the fully expanded fifth leaf and preserved in 70% formalin-acetic acid-alcohol (FAA) solution for 48h and then stored in 70% (v/v) aqueous ethanol. The samples were embedded in historesin (Leica Microsystems, Wetzlar, Germany) and sectioned in ~5 µm slices (RM 2155 Automated Microtome, Leica). Images obtained in a light microscope (Zeiss, Axioscope A1 model, Thornwood, NY, USA) with attached Axiovision® 105 color image capture system, were evaluated in the Image Pro-Plus® software (version 4.5, Media Cybernetics, Silver Spring, USA). All measurements were made in area of ~200 mm^2.

Gas exchange and chlorophyll fluorescence determinations

Gas exchange analyses were performed in MT and M82 plants at 50 and 40 days after germination, respectively, using terminal leaflets of fully expanded fifth leaf. Gas exchange measurements were performed simultaneously with chlorophyll *a* fluorescence measurements in the interval from 7:00 am to 12:00 am, for three consecutive days, using an open-flow gas exchange system infrared gas analyzer (IRGA) model LI-6400XT coupled with a fluorescence chamber (LI-Cor, Lincoln, NE, USA). All measurements were made on terminal leaflets of intact, attached leaves in the greenhouse. The analyses were performed under common conditions for photon flux density (1000 μmol m^{-2} s^{-1}, from an LED source), leaf temperature (25 ± 0.5ºC), leaf-to-air vapor pressure difference (16.0 ± 3.0 mbar), air flow rate into the chamber (500 μmol s^{-1}) and reference CO_2 concentration of 400 ppm (injected from a cartridge), using an area of 2 cm^2 in the leaf chamber. Intrinsic transpiration efficiency (TE_i) was calculed as the ratio between *A* and g_s. The dark respiration (R_d) determination was performed using an open-flow gas exchange system infrared gas analyzer (IRGA) model LI-6400XT coupled with a fluorescence chamber (LI-Cor, Lincoln, NE, USA), however, the plants were adapted to the dark at least 1h before the measurements, as described by Niinemets et al., 2006. Gas exchange parameters were carried out in eight plants per tretment.

Photochemical efficiency of photosystem II (φPSII) was determined in six replicates, by measuring the steady-state fluorescence (Fs) and the maximum fluorescence (F_m'), using a pulse of saturating light of approximately 8000 μmol photons m^{-2} s^{-1}, as described by Genty et al. (1989). The electron transport rate (ETR) was calculated as:

$$ETR = \varphi PSII \times \beta \times \alpha \times RFA$$

Where α is the absorbance of the sheet and β reflects the partitioning of the energy packets between photosystems I and II, and αβ was determined according to Valentini et al. (1995), from the relationship between *A* and RFA x φPSII / 4

obtained by varying the light intensity under non-photorespiratory conditions. The initial fluorescence emission (F_0) was determined illuminating dark-adapted leaves (1 h) with weak modulated measuring beams (0.03 μmol m^{-2} s^{-1}). A saturating white light pulse (8000 μmol m^{-2} s^{-1}) was applied for 0.8 s to obtain the maximum fluorescence (F_m), from which the variable-to-maximum Chl fluorescence ratio, was then calculated:

$$F_v/F_m=[(F_m - F_0)/F_m)]$$

In light-adapted leaves, the steady-state fluorescence yield (F_s) was measured with the application of a saturating white light pulse (8000 μmol m^{-2} s^{-1}) to achieve the light-adapted maximum fluorescence (F_m'). Far-red illumination (2 μmol m^{-2} s^{-1}) was applied after turning off the actinic light to measure the light-adapted initial fluorescence (F_0'). The capture efficiency of excitation energy by open photosystem II reaction centers (F_v'/F_m') was estimated following (Genty et al., 1989). We further measured the coefficients of photochemical (*qP*) and non-photochemical (*NPQ*) quenching and calculated electron transport (ETR) rates (Maxwell e Johnson, 2000)

A/C_i curves were determined initiated at an ambient [CO_2] of 400 μmol mol^{-1} under a saturating *PPFD* of 1000 μmol m^{-2} s^{-1} at 25°C under ambient O_2 supply. CO_2 concentration was decreased to 50 μmol mol^{-1} of air in step changes. Upon the completion of the measurements at low C_a, C_a was returned to 400 μmol mol^{-1} of air to restore the original *A*. Next, CO_2 was increased stepwise to 1600 μmol mol^{-1} of air. The A/C_i curves thus consist of *A* values corresponding to 12 different ambient CO_2 values. The maximum rate of carboxylation (V_{cmax}), maximum rate of carboxylation limited by electron transport (J_{max}) and triose-phosphate utilization (TPU) were estimated by fitting the mechanistic model of CO_2 assimilation proposed by (Farquhar et al., 1980). Corrections for the leakage of CO_2 into and out of the leaf chamber of the LI-6400 were applied to all gas-exchange data as described by Rodeghiero et al. (2007). A/C_i curves were determined in four replicates, using fourth fully expanded leaf.

Water relations

Leaf water potential (Ψ_w) was measured in the central leaflet of the fifth fully expanded leaf in MT and M82 plants 50 and 40 days of age, respectively, using a Scholander-type pressure chamber (model 1000, PMS Instruments, Albany, NY, USA). The apparent hydraulic conductance (K_{leaf}) determinations were performed simultaneously as the Ψw, and their value was estimated using the transpiration rates and the water potential difference between the transpiring and non-transpiring leaflet. The non-transpiring leaflet consisted of the lateral leaflet of the same leaf, which was covered with plastic film and foil the night before the measurements. K_{leaf} was calculated according to Ohm's law:

$$K_{leaf} = E / (\Psi_L - \Psi_X)$$

Where: E is the transpiration rate (mmol m^{-2} s^{-1}) determined during gas exchange measurements, and (Ψ_L - Ψ_X) corresponds to the pressure gradient between the transpiring and non-transpiring leaflet (MPa). Measurements of leaf water potential (Ψw) and hydraulic conductance were performed immediately after analysis of gas exchange. The number of replicates for this parameter was three and five for MT and M82 plants, respectively.

Biochemical determinations

The biochemical composition of the leaves were examined in MT and M82 plants 50 and 40 days after germination, respectively. The terminal leaflet of the sixth fully expanded leaf was collected around midday on a cloudless day, instantly frozen in liquid N_2 and stored at -80°C. Subsequently, the samples were lyophilized at -48°C and macerated with the aid of metal beads in a Mini-Beadbeater-96 type cell disrupter (Biospec Products, Bartlesville, OK, USA). The quantification of glucose, fructose and sucrose were performed according to Fernie et al. (2001). Quantification of the sugars was obtained indirectly from the absorbance of NADPH

formed as the enzymes glucose-6-phosphate dehydrogenase (G6PDH), hexokinase, phospho-glucose-Isomerase (PGI) and invertase were added to the reaction. The readings were made in Versamax ELISA microplate reader (Molecular Devices, Sunnyvale, CA, USA) at a wavelength of 340 nm using a 96-well plate. Protein and starch contents were determined from the precipitate (pellet) resulting from the extraction process with methanol and chloroform as described above. The readings were made at a wavelength of 595 nm. Pigment contents were obtained through the methodology proposed by Wellburn, (1994). The readings were made on a Versamax ELISA microplate reader (Molecular Devices, Sunnyvale, CA, USA) at 470, 653 and 666 nm using a 200 µl volume of the sample diluted in methanol in a ratio of 1:20 (v/v). For proteins, starch and sugars contents, four replicates were made per treatment, while for pigments, six replicates were given.

Agronomic parameters (yield and Brix)

Fruit agronomic parameters were determined in MT and M82 plants 80 days after germination. The number of fruits per plant was obtained from fruit counts and the frequency of green and mature fruits was also determined separately. The yield fruits per plant was obtained after weighing all fruits, using a semi analytical balance with a sensitivity of 0.01 g (AUY220, Shimadzu, Kyoto, Japan). Quantification was performed in six plants per treatment. The determination of the soluble solids content (°Brix) in the fruits was measured In five fruits per plant (in six plants) with a digital temperature-compensated refractometer, model RTD 45 (Instrutherm®, São Paulo, Brazil). Six ripe fruits per plant were evaluated in five replicates per genotype.

Statistical analysis

The data were subjected to analysis of variance (ANOVA) using Assistat version 7.6 (http://assistat.com) and the means were compared by the Tukey test at the 5% level of significance ($P \leq 0.05$).

Results

Initially we performed a microscopic analysis of terminal leaflet cross-sections to confirm that tomato cv. Micro-Tom (MT) harbors bundle sheath extensions (BSEs) in the translucent major veins of fully-expanded leaves (Figure S2). The *obscuravenosa* (*obv*) mutant, on the other hand, lacks these structures altogether. We therefore use the established nomenclature 'heterobaric' for MT and 'homobaric' for *obv*.

Growth irradiance alters leaf hydraulic conductance (K_{leaf}) in heterobaric but not in homobaric leaves

Leaf hydraulic conductance (K_{leaf}) is a key parameter determining plant water relations, as it usually scales up to the whole plant level. It is a measure of how much water loss through transpiration a leaf can sustain at a given water potential. In a previous work we showed that K_{leaf} is reduced in the homobaric mutant *obv* compared to MT (Zsögön et al., 2015). Here, we assessed K_{leaf} in heterobaric and homobaric leaves of two different tomato cultivars: the dwarf cultivar Micro-Tom (MT), and the commercial cultivar M82, grown in sun/shade conditions (Figure 1A). Shading decreased K_{leaf} in the heterobaric genotype: MT shade leaves had 41% lower K_{leaf} than sun leaves (14.95 ± 1.91 *vs* 25.36 ± 1.32 mmol H_2O m^{-2} s^{-1} MPa^{-1}). The *obv* mutant, on the other hand, showed similarly low K_{leaf} values in either condition, both comparable to the value of MT shade leaves (Figure 1B). This result was consistent in M82 (Figure 1), where shade leaves had 36% lower K_{leaf} than sun leaves (18.72 ± 0.59 *vs* 29.6 ± 2.1 mmol H_2O m^{-2} s^{-1} MPa^{-1}). The ranking was consistent between tomato backgrounds, even though both cultivars differ in leaf lamina size and other leaf structural parameters.

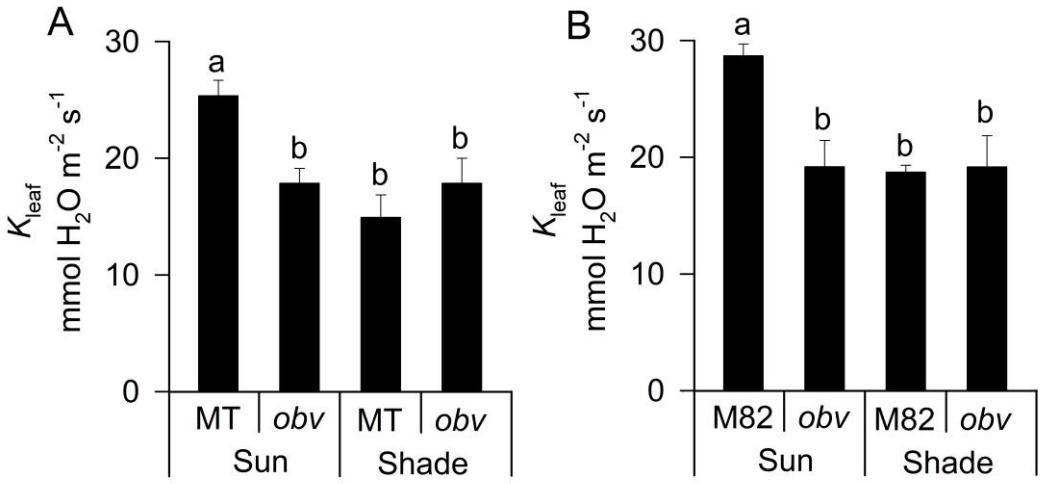

Figure 1. Tomato homobaric leaves show reduced hydraulic conductance (K_{leaf}) compared to heterobaric leaves when grown in the sun, but not in the shade. (A) Leaf hydraulic conductance in cv Micro-Tom (MT, heterobaric) and the *obscuravenosa* mutant (*obv*, homobaric) leaves from plants grown in either sun or shade conditions. (B) The same measurement but in tomato cv M82 compared to its isogenic line *obv*. Bars are mean values ± s.e.m. (n=3 for A and n=5 for B). Different letters indicate significant differences by Tukey's test at 5% probability.

Irradiance level alters leaf shape and structural parameters differentially in heterobaric and homobaric leaves

To analyse the structural and physiological basis of the differential response of K_{leaf} to irradiance between heterobaric and homobaric leaves, we conducted an analysis of leaflet shape between the treatments. We used an Elliptical Fourier Descriptor (EFD) analysis to determine how light treatment and the *obv* mutation affect leaf shape, independent from size. This method treats a closed contour as a wavelength that is decomposed into a Fourier harmonic series to quantify shapes (Iwata et al., 1998; Iwata e Ukai, 2002). A Principal Component Analysis (PCA) on harmonic coefficients contributing to symmetric shape variation separates MT and *obv* genotypes, but fails to show large differences in shape attributable to light treatment (Figure 2A). To visualize the effects of genotype and light, we superimposed mean leaflet shapes from each genotype-light combination (Figure 2B). *obv* imparts a wider leaflet shape relative to MT, regardless of light treatment. Light treatment does not discernibly affect leaflet shape.

These results are similar to previous studies in tomato and wild relatives in which the effects of the shade avoidance response on leaf shape were negligible compared to genotypic effects (Chitwood et al., 2012; 2015). Sun leaves had reduced total leaf area compared to shade leaves in both MT and the *obv* mutant (Figure 2C). The difference was, however, greater in *obv* than in MT. Results were similar for SLA (Figure 2D), as there was no significant difference in the dry weight of leaves between genotypes or treatments (Figure 2E). Shading increased SLA values by 101% and 62% for MT and *obv* plants, respectively, when compared to plants in the sun treatment (P=0.0001).Terminal leaflets of fully expanded MT sun leaves had 62% higher perimeter/area than MT shade leaves, unlike *obv* where no significant difference was found between irradiance levels (Figure 2F). Perimeter^2/area, which, unlike perimeter/area is a size-independent measure of leaf shape, was strongly dependent on genotype and not influenced by irradiance (Figure 2G). Leaf lamina thickness was greater in sun than in shade leaves, with no significant differences between genotypes (Figure 2H).

Gas exchange and chlorophyll fluorescence parameters in sun/shade heterobaric and homobaric leaves

Biochemical and stomatal limitations to photosynthesis can be partitioned by constructing A/C_i curves, *i.e.* the response of leaf CO_2 uptake to the intercellular mole fraction of CO_2. Key biochemical kinetic parameters that determine photosynthetic rate can be derived from such an analysis. We performed gas exchange measurements on fully expanded terminal leaflets attached to plants growing in the greenhouse under sun or shade treatments (Figure S3, Table 2). The apparent maximum carboxylation rate of Rubisco (V_{cmax}), the maximum rate of electron transport used in the regeneration of RuBP (J_{max}) and the speed of use of trioses-phosphates (TPU) were reduced by ~20% (P=0.0696), 20% (P = 0.01) and ~21% (P = 0.006), respectively, for shade compared to sun MT plants. In *obv*, the respective drop between sun and shade plants the same parameters was 10%, 7% and 6% respectively (Table 2).

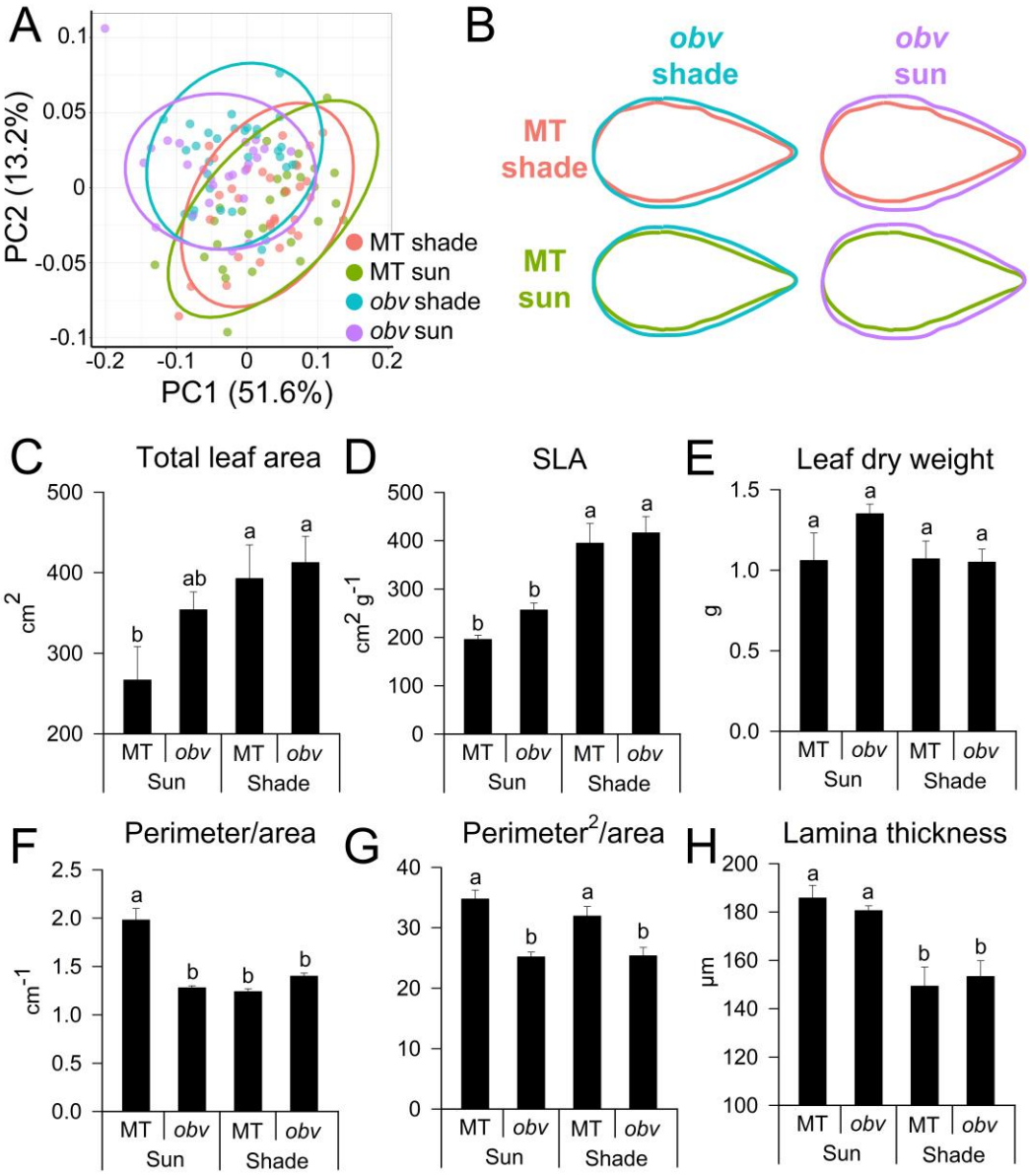

Figure 2. Growth irradiance level differentially alters morphology in heterobaric and homobaric leaves. A) Principal Component Analysis (PCA) on A and D harmonic coefficients from an Elliptical Fourier Descriptor (EFD) analysis shows distinct symmetric shape differences between MT and *obv* leaflets, but small differences due to light treatment. 95% confidence ellipses are provided for each genotype and light treatment combination, indicated by color. B) Mean leaflet shapes for MT and *obv* in each light treatment. Mean leaflet shapes are superimposed for comparison. Note the wider *obv* leaflet compared to MT. MT shade, red; MT sun, green; *obv* shade, blue; *obv* sun, purple. Morphological parameters: C) Total leaf area; D) specific leaf area (SLA); E) leaf dry weight; F) relationship between perimeter/area; G) perimeter^2/area, and H) leaf lamina thickness determined microscopically from cross-sections. Bars are mean values ± s.e.m. (n=5). Different letters indicate significant differences by Tukey's test at 5% probability.

Table 2. Gas exchange parameters determined in fully-expanded leaves of heterobaric (Micro-Tom, MT) and homobaric (*obscuravenosa*, *obv*) in two irradiance levels (sun/shade, 900/300 µmol photons m^{-2} s^{-1}). Values are means ± s.e.m (n=8 for A, g_s and TE_i; n=4 for other parameters). Values followed by the same letter were not significantly different by Tukey test at 5% probability.

	Sun		**Shade**	
	MT	***obv***	**MT**	***obv***
A (µmol CO_2 m^{-2} s^{-1})	21.29 ± 1.34a	20.74 ± 1.44a	17.07 ± 0.83b	20.26 ± 0.48a
g_s (mol m^{-2} s^{-1})	0.373 ± 0.039a	0.275 ± 0.020b	0.263 ± 0.016b	0.278±0.018b
TE_i (A/g_s)	59.16 ± 3.25b	76.26 ± 2.16a	65.51 ± 2.08b	74.11 ± 3.55a
$V_{c,max}$ (µmol m^{-2} s^{-1})	82.7 ± 6.04a	80.5 ± 6.26a	66.8 ± 4.38a	72.7 ± 7.72a
J_{max} (µmol m^{-2} s^{-1})	167.5± 5.74a	155.5 ± 8.48a	133.5 ± 4.54b	133.5 ± 4.54b
TPU (µmol m^{-2} s^{-1})	12.1 ± 0.34a	11.0 ± 0.62a	9.6 ± 0.36b	10.3 ± 0.1a
R_d (µmol CO_2 m^{-2} s^{-1})	1.49 ± 0.43 a	1.80 ± 0.45 a	1.42 ± 0.38 a	1.45±0.39a

The hyperbolic relationship between A and g_s measured at ambient CO_2, was not altered by irradiance level (Figure 3). The lower limit for g_s values was remarkably similar between genotypes in both light conditions (~0.2 mol m^{-2} s^{-1}). Shading, however, drove a 30% decrease in g_s in MT (P= 0.029) with a concomitant limitation to A (P=0.023) (Table 2), mostly by reducing the variability for this parameter in MT (Figure 3). In the *obv* mutant, g_s was lower in the sun (similar value to shade MT) and remained essentially unchanged by shading (P=0.9293), as did A (P=0.6350). The A/ g_s ratio, or intrinsic transpiration efficiency (TE_i), was therefore higher in homobaric *obv* plants than in heterobaric MT under both irradiance levels. A similar, although not statistical significant difference (possibly owing to the lower number or replicates, n=5) was found in M82 (Figure S4).

The chlorophyll fluorescence analyses did not reveal any significant differences between genotypes in the photosynthetic efficiency of light utilisation (Table S1).

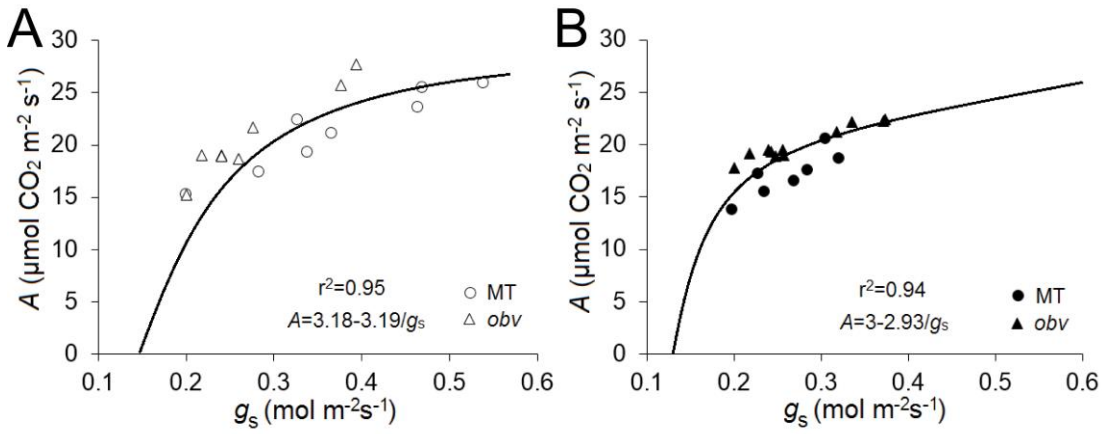

Figure 3. Relationship between photosynthetic CO_2 assimilation rate (A) and stomatal conductance (g_s) for Micro-Tom (MT) and the *obscuravenosa* (*obv*) mutant plants grown in the sun (A) or shade (B). A rectangular hyperbolic function was fitted in each panel. Each point corresponds to an individual measurement.

Stomatal traits in heterobaric and homobaric leaves under different irradiance

Stomatal conductance (g_s) is determined by the maximum stomatal conductance (g_{max}), which is in turn determined by stomatal size and number. To further explore the basis for the differential response to irradiance of g_s between genotypes, we analysed stomatal traits in terminal leaflets of fully expanded leaves. Stomatal index, the proportion of guard cells to total epidermal cells, was similar across treatments for the abaxial side (Figure 4A) but strongly reduced by shading (61.7% reduction for MT and 72.8% for *obv* in comparison with their respective sun counterparts) on the adaxial side of the leaf (Figure 4B). The proportion of stomata in the abaxial side of the leaf (between 76% and 91%) was maintained across treatments. Stomatal pore index area (SPI, a dimensionless measure of the combined stomatal density and size) was increased in MT sun leaves (Figure 4C), but not in *obv* sun leaves, where it was within the same range of both genotypes grown in the shade. Guard cell length, which is linearly related to stomatal pore radius, was greater in *obv* than in MT and was not significantly affected by the irradiance levels (Figure 4D). Thus, the main driver of the difference in SPI was stomatal density, particularly in the abaxial side, which represents a quantitatively large contribution

(Figure 4E). Adaxial stomatal density was significantly reduced in the shade for both genotypes, with no differences between them within irradiance levels (Figure 4F). The size epidermis pavement cell area (Figure 4G) was significantly higher for the *obv* mutant compared to MT in both irradiance conditions, as well as on the adaxial side (Figure 4H).

Irradiance levels and anatomical traits in heterobaric and homobaric leaves

Cross-sectional analysis of leaves revealed differences in leaf anatomy dependent on genotype and irradiance level. As shown above (Figure 2H), lamina thickness was reduced by shading in both genotypes, with no significant difference between them (Figure 5A). Palisade parenchyma thickness was remarkably stable across genotypes and light conditions (Figure 5C), whereas spongy parenchyma was reduced in both genotypes in the shade (Figure 5D), with a concomitant increase in the palisade/spongy parenchyma ratio (Figure 5E). Thickness of the abaxial epidermis, a proxy for stomatal depth, did not vary in MT between irradiances, but was significantly reduced in shaded *obv* plants (Figure 5F). Intercellular air spaces in the lamina comprised close to 10% of the cross-sectional area in sun MT and *obv*, but was increased to 12.98% (P=0.0658) in MT and 17.75% (P=0.0036) in *obv* (Figure 5G). Venation is a key trait that influences water distribution in the lamina, we assessed minor vein density (tertiary and higher orders) and observed a significant genotype×irradiance interaction (Figure 5B). Vein density was reduced in both genotypes by shading, but more strongly in MT than in *obv* (Figure 5H).

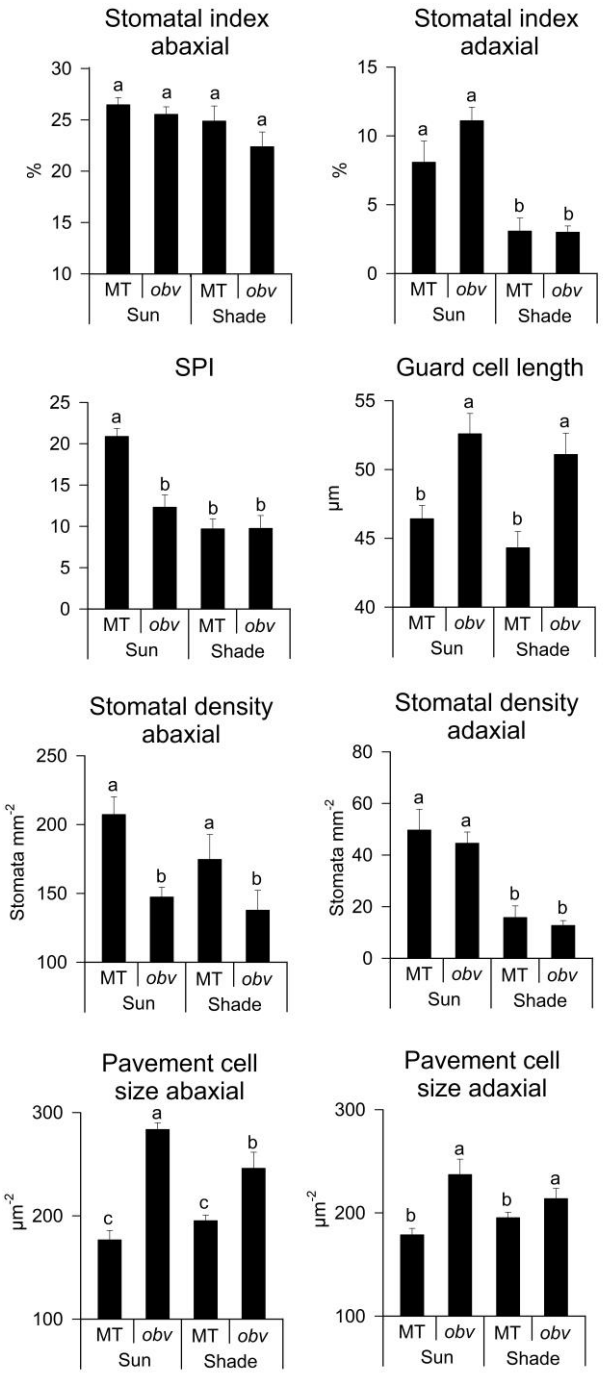

Figure 4. Stomatal traits are differentially affected by irradiance in heterobaric and homobaric tomato leaves. (A)-(B) Stomatal index, the proportion of stomatal to total cells in the epidermis, expressed as percentage of total cells; (C) SPI: stomatal pore index, calculated as (guard cell length)^2 × stomatal density for the adaxial and abaxial epidermes and then added up; (D) Guard cell length; (E)-(F) Stomatal density, number of stomata per unit leaf area (in ~200 mm^2); (G)-(H) epidermis pavement cell area. All histograms show mean values ± s.e.m. (n=6).

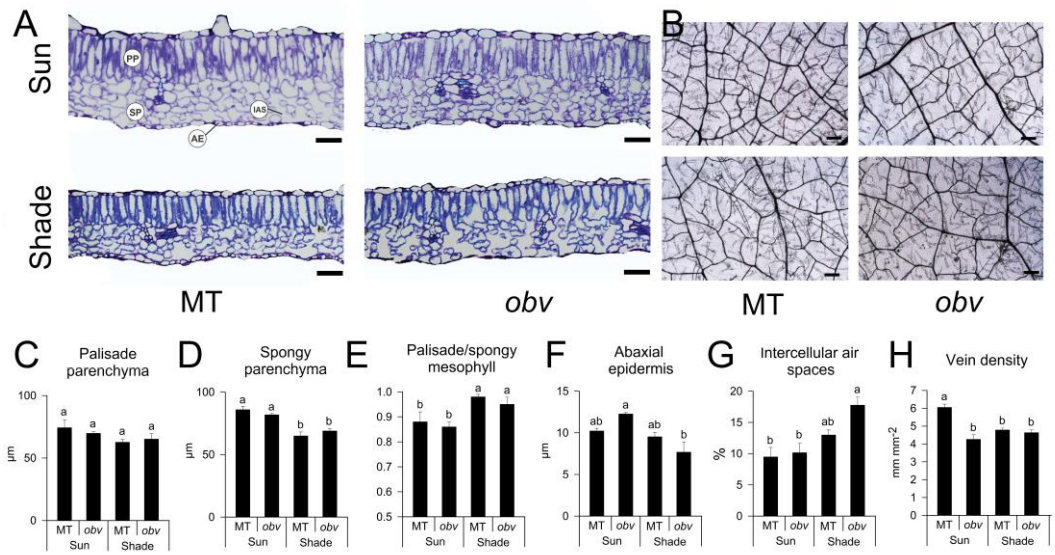

Figure 5. Irradiance level differentially alters leaf anatomical parameters in heterobaric and homobaric leaves. (A) Representative cross-sections of tomato cv Micro-Tom (MT, heterobaric) and the *obscuravenosa* mutant (*obv*, homobaric) leaves from plants grown in either sun or shade. The background was removed for clarity. PP: palisade parenchyma; SP: spongy parenchyma; IAS: intercellular air spaces; AE: abaxial epidermis. All leaf cross-section parameters were measured in ~200 mm^2. (B) Plates showing the pattern and density of minor veins in 7.8 mm^2 sections in mature, cleared leaves. Scale bar=200 µm. (C)-(H) Histograms with mean values ± s.e.m. (n=6) for thickness of palisade and spongy parenchyma; the ratio between the two; thickness of the abaxial epidermis; the proportion of intercellular air spaces and the density of minor (quaternary and higher order) veins measured in cleared sections of the leaves.

Protein, carbohydrate and pigment contents in heterobaric and homobaric leaves under different irradiance

Leaf traits related to carbon economy are generally not strongly coordinated with leaf hydraulic traits. To ascertain whether the anatomical and physiological differences described above impacted leaf biochemistry, we assessed a basic set of compounds related to primary cell metabolism in MT and *obv* under both sun and shade conditions, along with photosynthetic pigments (Table 3). Soluble protein is a proxy for Rubisco content, which represents around 90% of the total soluble protein in the leaf. Protein levels were higher in shaded plants and significantly (P=0.03) higher in *obv* than in MT in the shade. As expected, carbohydrate concentrations were strongly matched with irradiance level (Table 3). Shading promoted a significant (P=0.001) decrease in starch content in shaded leaves of both genotypes, but of a considerable greater magnitude in MT (-45%) than in *obv* (-28.5%)

compared to sun plants (Table 3). Higher levels of total soluble proteins were observed for shade compared to sun plants (*P*=0.005), but the increase was stronger in MT (110%) than in *obv* (57%). Glucose and fructose were increased in the shade, with no difference between genotypes. We next evaluated the levels of photosynthetic pigments in leaves of MT and *obv* plants in sun and shade treatment. No significant difference was found between genotypes for chlorophyll *a* (Chl *a*) values, but shading increased the levels of this pigment for by 121% MT plants and 80% for *obv* (*P*=0.0001), compared to the sun plants. *obv* shade plants presented a 100% increase in chlorophyll *b* (Chl *b*) levels, compared to their sun counterparts (*P*=0.002), however, this increase was not observed for MT plants under this same condition The chlorophyll *a/b* ratio was similar for all plants (*P*=0.24). A slight increase in carotenoid (CAR) levels was found in *obv* shade plants (*P*=0.004) (Table 3).

Table 3. Leaf carbohydrate and pigment contents evaluated 50 days after germination (dag) in heterobaric tomato (Micro-Tom, MT) and homobaric (*obscuravenosa*, *obv*) plants grown in two irradiance levels (sun/shade, 900/300 µmol photons m^{-2} s^{-1}). Samples were collected at 12:00 h. Values are means ± s.e.m (n=4 for protein and carbohydrates, n=6 for pigments). Values followed by the same letter were not significantly different by Tukey test (P <0.05).

	Sun		**Shade**	
	MT	***obv***	**MT**	***obv***
Soluble protein (µg mg^{-1} DW)	44.31 ± 7.95c	78.00 ±	93.4 ± 5.57b	122.89 ±
Carbohydrates				
Starch (µmol g^{-1} DW)	245.21 ±	288.24 ±	134.08 ±	209.49 ± 4.18b
Sucrose (µmol g^{-1} DW)	17.85 ± 2.28a	22.80 ± 2.79a	27.23 ± 1.02a	33.02 ± 6.74a
Glicose (µmol g^{-1} DW)	22.94 ± 3.44b	20.23 ± 4.07b	46.51 ± 2.81a	45.97 ± 1.30a
Fructose (µmol g^{-1} DW)	4.69 ± 0.48b	4.35 ± 0.53b	9.17 ± 0.24a	8.70 ± 1.28a
Pigments				
Chlorophyll a (mg g^{-1} DW)	2.02 ± 0.52c	3.48 ± 0.75bc	4.46 ± 0.41ab	6.29 ± 0.22a
Chlorophyll b (mg g^{-1} DW)	1.40 ± 0.53b	1.59 ± 0.36b	2.16 ± 0.24ab	3.19 ± 0.14a
Total chlorophyll (mg g^{-1}	3.42 ± 0.97c	5.08 ± 1.11bc	6.62 ± 0.65b	9.49 ± 0.36a
Chlorophyll a/b ratio	1.82 ± 0.28a	2.21 ± 0.07a	2.10 ± 0.08a	1.97 ± 0.03a
Carotenoids (mg g^{-1} DW)	0.29 ± 0.06b	0.43 ± 0.09ab	0.49 ± 0.07ab	0.70 ± 0.06a

Morphological differences between heterobaric and homobaric plant grown under different irradiances does not affect dry mass accumulation or fruit yield

To determine whether the differences shown above scale up to the whole-plant level and affect carbon economy and agronomic parameters of tomato, we determined dry mass and fruit yield in sun and shade grown plants of MT and *obv*. MT and *obv* plants grown in sun or shade are shown in the inset of Table 4. There was no difference in plant height (P=0.82) or in the number of leaves before the first inflorescence (P=0.82), for plants of either genotype in both light intensities (Table 4). Leaf insertion angle relative to the stem, however, was steeper in the *obv* mutant under both irradiance conditions. There was a decrease of 29% and 26% in stem diameter in MT and *obv* plants respectively, for the shade treatment compared to sun (P=0.001). Different light intensities did not change leaf dry weight (P=0.25), however, *obv* plants showed a 24% reduction in stem dry weight (P=0.006), 46% in root dry weight (P=0.0002) and 31% in total dry weight (P=0.01) when compared to the sun treatment. The results were similar for MT, so no changes in dry mass allocation pattern were discernible between genotypes. Side branching is one of the most common gross morphological parameters affected by shading. A significant decrease (P=0.0001) in side branching was found in both genotypes, with no significant differences between them (Figure S5). Different light intensities did not change leaf dry weight (P=0.25), however, *obv* plants showed a 24% reduction in stem dry weight, under conditions of shade when compared to sun treatment (P=0.006). Shading reduced 46% of root dry weight in *obv* plants in compared to the same plants grown in the sun (P=0.0002). Total dry weight of the mutant plants was reduced 31% under low light intensity (P=0.01).

The results described in this section revealed that vegetative dry mass accumulation was affected solely by irradiance level with no influence of the genotype (and therefore of the BSE). To ensure that potential differences arising from altered partitioning or allocation of carbon were not overlooked, we also assessed reproductive traits, *i.e.* parameters related to tomato fruit yield. Average

tomato fruit yield per plant was significantly reduced by shading, but did not differ between genotypes within each irradiance condition (Table S2). The content of soluble solids in the fruit (Brix), a parameter of agronomic interest, was consistently stable across genotypes and treatments.

Table 4. Plant morphological parameters evaluated 50 days after germination (dag) in heterobaric (Micro-Tom, MT) and homobaric (*obscuravenosa*, *obv*) tomatoes grown in two irradiance levels (sun/shade, 900/300 µmol photons m^{-2} s^{-1}) (n=8). Dry weight was determined through destructive analysis in plants 65 dag (n = 5). Values followed by the same letter were not significantly different by

	Sun		Shade	
	MT	***obv***	**MT**	***obv***
Plant height (cm)	9.90 ± 0.30a	10.53 ± 0.28a	10.15 ± 0.62a	10.63 ± 0.18a
Leaves to 1st	6.75 ± 0.25a	6.50 ± 0.18a	6.62 ± 0.18a	6.75 ± 0.25a
Leaf insertion angle (°)	82.8 ± 2.32a	73.1 ± 3.50b	81.8 ± 4.30a	65.5 ± 3.72b
Stem diameter (cm)	0.40 ± 0.02a	0.38 ± 0.03a	0.28 ± 0.01b	0.28 ± 0.01b
Dry weight (g)				
Leaves	1.30 ± 0.17a	1.35 ± 0.06a	1.07 ± 0.11a	1.05 ± 0.08a
Stem	2.17 ± 0.14ab	2.49 ± 0.19a	1.54 ± 0.18b	1.72 ± 0.07a
Roots	0.80 ± 0.06a	0.80 ± 0.04a	0.50 ± 0.03b	0.43 ± 0.04b
Total	4.28 ± 0.34ab	4.65 ± 0.28a	3.12 ± 0.32b	3.21 ± 0.14b

Discussion

A limitation in the study of the coordination of leaf structural and physiological traits is that most of the work on the topic has been conducted addressing interspecific level relations, with less work published at the intraspecific level. Many simple and relevant trait-trait correlations are potentially obscured by the analysis of multi-species mean values (Lloyd et al., 2013). Breaking down individual traits within single species of a given life form and then adding up their contributions is an alternative. Available mutants in model organisms are a suitable material for such an approach (Carvalho et al., 2011). Here, we compared different

genotypes of a single herbaceous species (tomato) varying for a defined and ecologically relevant structural feature of the leaves: the presence of bundle sheath extensions (BSEs). The mutant *obscuravenosa* (*obv*) lacks BSEs and thus produces homobaric leaves, compared to Micro-Tom (MT) tomatos, which have heterobaric leaves (Zsögön et al., 2015). In this work we also extended these observations to a different tomato cultivar, M82, which, unlike Micro-Tom (MT), is not a *dwarf* plant. This is relevant because the MT leaf is characteristically wrinkled as a result of its relatively low brassinosteroid content (Marti et al., 2006). We assessed the effect that growing plants on two contrasting levels of irradiance on a series of developmental and physiological parameters. We hypothesized that homobaric leaves, lacking a key physical feature that increases leaf hydraulic integration, would exhibit less plasticity in their response to environmental conditions than heterobaric leaves. It was predicted that, under varying irradiance, homobaric leaves would not acclimate either structurally and/or physiologically to the same degree as heterobaric leaves.

K_{leaf} was higher in heterobaric than in homobaric sun plants, as BSEs act as an additional extra-xylematic pathway for the flow of liquid water (Buckley et al., 2011; Zsögön et al., 2015). K_{leaf} is dynamically influenced by irradiance over different time scales, in the short-term dynamically due to yet unknown factors (Scoffoni et al., 2008b), and in the long-term due to developmental plasticity altering leaf structural and physiological traits (Scoffoni et al., 2015). K_{leaf} was lower in shade- than sun-grown heterobaric plants, whereas homobaric shade plants showed similar values to their sun counterparts. Thus, the presence of BSEs affects leaf hydraulic architecture in response to irradiance. A direct biophysical effect can be responsible for these results. A possible role for aquaporins present in the BSE and/or the mesophyll has been proposed (Cochard et al., 2007). Alternatively, the presence of BSEs could be coordinated with the plastic response to irradiance of other leaf structural and physiological traits. We dissect some of these traits below.

Leaf venation pattern affects a large suite of hydraulic parameters, either directly and mechanistically (*e.g.* K_{leaf}) or indirectly through concerted developmental patterning and co-selection (*e.g.* stomatal density). Tomato exhibits an open reticulate venation pattern, and, unlike other apoplastic loading eudicots, responds to irradiance levels by altering vein density (Adams et al 2007). Reduced photosynthetic capacity in shade- compared to sun-grown plants has been attributed to a structural limitation imposed by low vein density limiting the total phloem loading surface. Plasticity for vein density under different irradiance levels has thus been proposed as a proxy for the flexibility of photosynthetic acclimation in either symplastic- or apoplastic-loading species. The significant reduction in minor vein density (fourth order and higher) and the concomitant drop in *A* and TPU observed in MT tomatoes concur with this idea. The homobaric mutant, however, responds differently. In the *obv* mutant, vein densities are low (*i.e.* as low as in heterobaric plants in the shade) in either sun- or shade-grown plants, but *A* and TPU remain similarly high nevertheless (*i.e.* as in heterobaric plants in the sun). Minor vein density is thus strongly and positively correlated with K_{leaf} across treatments and, along with the presence/absence or BSEs, coordinates water flux through the leaf together with stomatal density.

Stomatal conductance (g_s) responds to irradiance, relative humidity, soil water content and ambient CO_2 levels (Assmann, 1999; Mott, 2007; Shimazaki et al., 2007; Mott & Peak, 2010). Modelling work predicts that g_s should increase with irradiance if water is not a limiting factor. Plants in sunny environments have an adaptive advantage from higher leaf maximum conductance (Mott et al., 1982). Anatomically, g_s is determined by stomatal size and number, which can be combined into a single parameter, stomatal pore area index (SPI) (Sack et al., 2003a). Here, SPI was affected by irradiance×genotype, as SPI in homobaric leaves did not respond to the change in growth irradiance, whereas SPI in the heterobaric genotype doubled in sun *vs* shade conditions. Tomato is considered a hypostomatic species, as a large proportion of stomata are located in the abaxial epidermis, but

irradiance can alter the ratio significantly (Gay & Hurd, 1975). The change in SPI was driven mostly by changes in stomatal density, rather than guard cell size, which was remarkably constant across light conditions (and higher for homobaric than heterobaric leaves). Stomatal density differences, in turn, are apparently the result of greater epidermal pavement cell expansion in homobaric leaves, in both adaxial and abaxial sides of the leaf.

Photosynthetic rates on an area basis (*A*) in response to irradiance levels depend on both biochemical and structural parameters (Terashima et al., 2001). Rubisco concentration and activity are the most determinant among the former (Carmo-Silva et al., 2015). Of the latter, leaf lamina thickness, leaf mass per area and mesophyll surface area are usually considered the most relevant. Leaf development is highly plastic to irradiance, sun leaves are thicker and more serrated (increased margin dissection) than shade leaves. Previous work has shown that at a given lamina thickness, heterobaric species have higher A_{area} rates than homobaric species. Here, we showed that homobaric tomato plants have higher *A* values than heterobaric plants when grown at low irradiance, but that in sun-grown plants *A* increases considerable more in heterobaric plants. Our 'sun' treatment consisted of intermediate irradiance levels (~900 μmol photons m^{-2} s^{-1} at midday), so it is possible that higher irradiance values could favor more significant increases in *A* in heterobaric plants compared to homobaric ones. Net photosynthesis in tomato approaches light saturation at 2200 μmol photons m^{-2} s^{-1}, with rates of ~40 μmol CO_2 m^{-2} s^{-1} (Bolaños e Hsiao, 1991).

We have also shown that the presence of bundle sheath extensions (BSEs) alters the coordination between lamina thickness and biochemical and structural parameters in response to different levels of irradiance. The response of lamina thickness itself to irradiance levels was not altered between genotypes with or without BSEs. Variation for soluble protein levels, a proxy for Rubisco content, was not significantly affected either, although the values were consistently higher for homobaric plants in both conditions. Lateral diffusion of CO_2 occurs through the

intercellular air spaces in the spongy parenchyma. The amount of intercellular air spaces is linearly related to the total surface area of chloroplasts facing the intercellular spaces per unit leaf area, and thus a determinant of the diffusional resistance within the leaf blade (Evans e vonCaemmerer, 1996). The plastic response in amount of intercellular air spaces to shading was markedly higher in homobaric than in heterobaric leaves. This could partly account for the higher *A* in homobaric than heterobaric leaves in the shade. Heterobaric leaves, on the other, responded strongly to irradiance in the amount of stomatal pores per unit leaf area (SPI), a parameter to which homobaric leaves were unresponsive. The developmental basis for this plasticity is not found in changes in the rate of stomatal development (stomatal index), which was consistently similar across treatments, but in the differential expansion of epidermal pavement cells. Another parameter affecting CO_2 diffusion is guard cell size, a proxy for stomatal pore diameter, which was significantly higher in homobaric than heterobaric leaves under both irradiance levels, and shower little variation in response to light treatment.

Taken together, the slopes of the reaction norms of the traits mentioned above point to a different direction of the plastic response in each genotype (Figure 6). Both tend to accumulate more soluble protein in response to shading, although homobaric leaves maintain higher levels across conditions. CO_2 diffusivity appears to be adjusted via intercellular air spaces in homobaric leaves and via stomatal and vein density in heterobaric ones. This is in accord to the fact that BSEs integrate the vascular system with the epidermis and the stomatal response. Sustaining higher *A* is possible for homobaric leaves under low irradiance, but the values equalize at intermediate irradiances. We hypothesize that heterobaric leaves will perform better at higher irradiances. Based on Sack and Scoffoni (2013), we propose a model whereby the presence of BSEs affects leaf plasticity in response to irradiance. A wide set of physiological and structural traits are known to shift in tandem in response to irradiance (Scoffoni et al., 2015). We propose that the presence of BSEs acts as a hub coordinating trait plasticity (Figure 7). In genotypes possessing BSEs,

irradiance alters mainly two parameters: SPI and minor vein density. This fits with the proposed role of BSEs as hydraulic communication routes between the vascular bundles and the epidermis (Zwieniecki et al., 2007). Plants lacking BSEs, on the other hand, maintain a higher soluble protein (hence, probably Rubisco) content and respond to irradiance by altering the amount of intercellular air spaces available for CO_2 diffusion. Given that homobaric leaves derive a physiological advantage from the gaseous integration of the leaf lamina (Pieruschka et al., 2006), it is unsurprising that their response to irradiance involves increased plasticity for a structural trait that increases intracellular CO_2 diffusivity (Flexas et al., 2013).

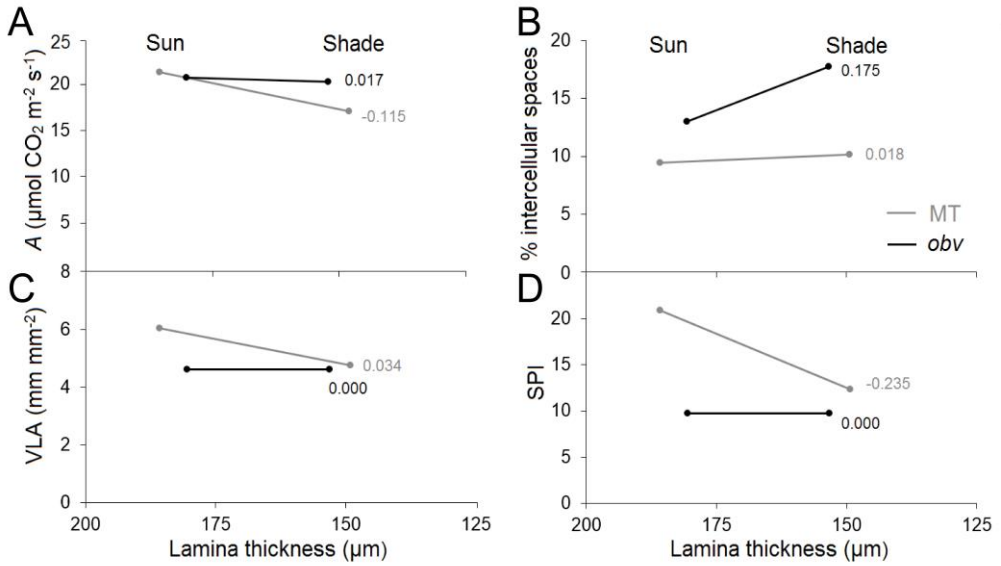

Figure 6. Reaction norms of structural and physiological traits in relation to leaf thickness in response to irradiance levels in homobaric and heterobaric leaves. (A) light-saturated photosynthetic assimilation rate (*A*); (B) proportion of intercellular air spaces in the lamina, (C) minor vein per unit leaf area (VLA) and (D) stomatal pore area index (adimensional). The values of the slopes are shown next to each line.

It is nevertheless difficult to ascertain whether the significant differences in physiological traits between genotypes in contrasting light environments are due to the presence/absence of BSEs or to correlative variation in other leaf structural traits mechanistically linked to BSEs. We see two complementary avenues for resolving this conundrum. One is exploring physiological acclimation upon transfer of sun-

grown plants to the shade and vice-versa, and therefore uncoupling structural traits from hydraulic responses to irradiance level. The other is determining the genetic basis for the production of BSEs, which is underway in our laboratory through molecular cloning of the *OBV* gene. When this is archieved, it will be possible to generate (a) novel allelic variation and therefore a wider range of phenotypes than the two currently available, and (b) inducible gene constructs which can be used to alter the ontogenetic trajectory of BSEs. Such a genetic toolkit to manipulate leaf developmental plasticity would greatly widen the scope of feasible experimental work, which has hitherto been restricted to relatively wide inter-specific comparison. Another open question is why the structural and physiological effects of the absence of BSEs in a leaf do not scale up to whole-plant growth and carbon economy. In other words, under what set of environmental conditions (if there is one) does the presence or absence of BSEs result in a significant fitness (*i.e.* survival and reproduction) difference between genotypes? The present work was limited to analyzing the effect of quantitative differences in irradiance and is thus only a starting point to answering this question. The strong plasticity of plant development in response to irradiance (all other conditions being similar) could be the reason why potential economic differences between genotypes were canceled out within a given light environment. It is not possible to rule out that stronger quantitative differences in irradiance level than the one tested here could tilt the phenotypic and fitness scales in favor of one of the leaf designs (*i.e.* heterobaric/homobaric). Alternatively, other variables (water, nitrogen availability, ambient CO_2 concentration) and combinations thereof could result in conditions where the difference in leaf structure scales up to the whole plant level. We endeavor to address these questions in the near future.

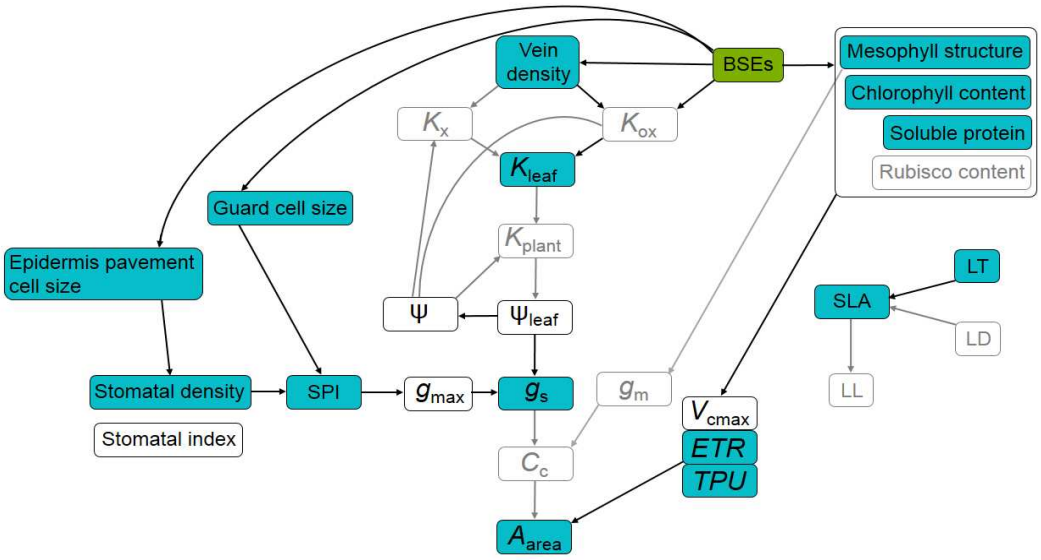

Figure 7. **Hypothetical model showing the influence of bundle sheath extensions (BSEs) on leaf plasticity for structural and physiological traits**. BSEs were the independent variable in this work (green). Traits affected the presence or absence of BSEs in response to changes in growth irradiance are shown in blue. Traits measured and not affected are shown in open boxes and traits not measured in this study are in grey. Vein density in our study refers to minor vein length per leaf area. K_x, K_{ox} hydraulic conductance in the xylem and outside the xylem, respectively. K_{leaf}, K_{plant}, leaf and plant hydraulic conductance. Ψ, water potential; Ψ_{leaf}, leaf water potential; g_{max}, maximum stomatal conductance; g_s, stomatal conductance; g_m, mesophyll conductance; C_c, chloroplastic CO_2 concentration; V_{cmax}, maximum CO_2 carboxylation rate; J_{max}, electron transport rate; SLA, specific leaf area; LT, LD, LL, leaf thickness, density and lifespan; SPI, stomatal pore area index. See text for detailed definitions of each parameter.

Conclusions

The presence of bundle sheath extensions (BSEs) in heterobaric tomato plants is coordinated with variation in leaf structural and physiological traits under different growth irradiance levels (sun/shade). A homobaric mutant where BSEs are absent shows a pattern of responses whereby the plastic response is shifted to a different set of traits than the one affected in heterobaric plants. This variation, nevertheless, allows homobaric plants to maintain leaf physiological performance and growth under both irradiance conditions and results in the carbon economy and allocation of either genotype being indistinguishable within each irradiance level.

Further insight into this fascinating complexity will come when the genetic basis for BSE development is unveiled.

Acknowledgments

This work was supported by funding from the Agency for the Support and Evaluation of Graduate Education (CAPES-Brazil), the National Council for Scientific and Technological Development (CNPq-Brazil), Foundation for Research Assistance of the São Paulo State (FAPESP-Brazil) and the Foundation for Research Assistance of the Minas Gerais State (FAPEMIG-Brazil). We thank CAPES for studentship granted to M.A.M.B. W.L.A. and L.E.P.P. acknowledge grants from CNPq (grant 307040/2014-3 to L.E.P.P.).

Supplementary information

Tables

Table S1. Chlorophyll fluorescence in tomato Micro-Tom (MT) and mutant *obv* in two irradiance levels (sun/shade, 900/300 µmol photons m^{-2} s^{-1}). F_v'/F_m', maximal quantum efficiency of photosystem II (PSII); F_v/F_m, quantum efficiency of PSII in dark-adapted leaves; ΦPSII, efficiency of PSII photochemistry; ETR, electron transport rate; *qP*, photochemical quenching coefficient; *NPQ*, non-photochemical quenching. Values are means ± s.e.m (n=6). Values followed by the same letter were not significantly different by Tukey test at 5% probability.

	Sun		**Shade**	
	MT	***obv***	**MT**	***obv***
F_v'/F_m'	0.534 ± 0.01b	0.582 ± 0.01a	0.574 ± 0.01a	0.574 ± 0.01a
F_v/F_m	0.788 ± 0.01a	0.760 ± 0.01a	0.787 ± 0.01a	0.787 ± 0.01a
ΦPSII	0.352 ± 0.02b	0.431 ± 0.02a	0.332 ± 0.03b	0.369 ± 0.01b
ETR	154.57 ±	189.33 ±	145.82 ± 14.21b	161.87 ± 6.92a
qP	0.657 ± 0.04ab	0.739 ± 0.02a	0.590 ± 0.04b	0.642 ± 0.01b
NPQ	1.619 ± 0.06a	1.326 ± 0.17a	1.562 ± 0.15a	1.494 ± 0.08a

Table S2. Total fruit yield averaged per plant and fruit total soluble content (Brix) in heterobaric (Micro-Tom, MT) and homobaric (*obscuravenosa*, *obv*) in two irradiance levels (sun/shade, 900/300 µmol photons m^{-2} s^{-1}). Values are means ± s.e.m (n=6). Values followed by the same letter were not significantly different by Tukey test at 5% probability.

	Sun		**Shade**	
	MT	***obv***	**MT**	***obv***
Yield (g)	74.34 ± 6.61a	68.44 ± 4.26a	20.32 ± 1.50b	17.40 ± 1.55b
Brix	4.47 ± 0.34a	4.12 ± 0.13a	4.22 ± 0.07a	4.47 ± 0.12a
	M82	***obv***	**M82**	***obv***
Yield (g)	1537 ± 114a	1451 ± 140a	805 ± 82b	666 ± 136b
Brix	5.12 ± 0.40a	5.04 ± 0.45a	4.88 ± 0.35a	4.15 ± 0.18a

Figures

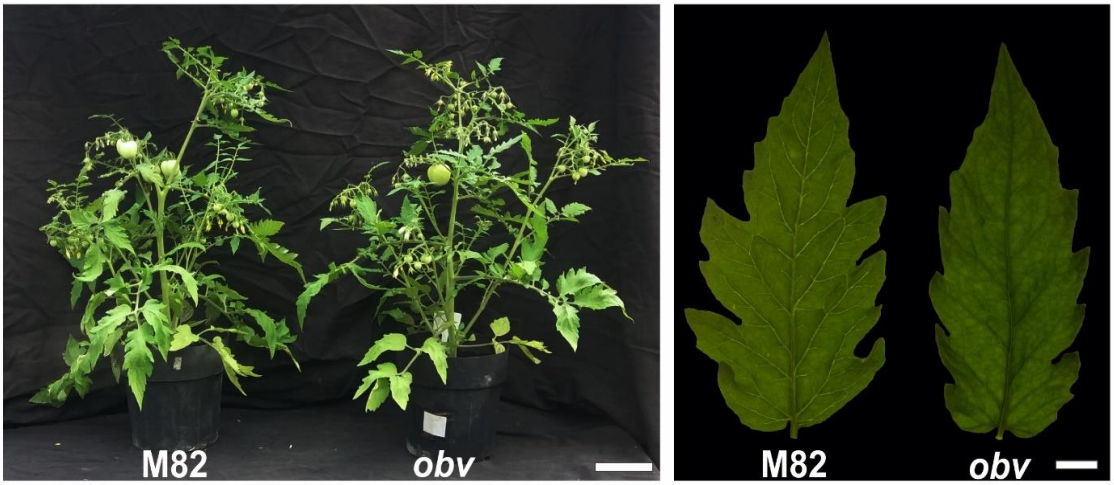

Figure S1. Representative F1 plants and terminal leaflets of Micro-Tom × M82 ("M82") and Micro-Tom *obv* × M82 ("*obv*"). Scale bars= 10 cm (pots) and 1 cm (leaflets).

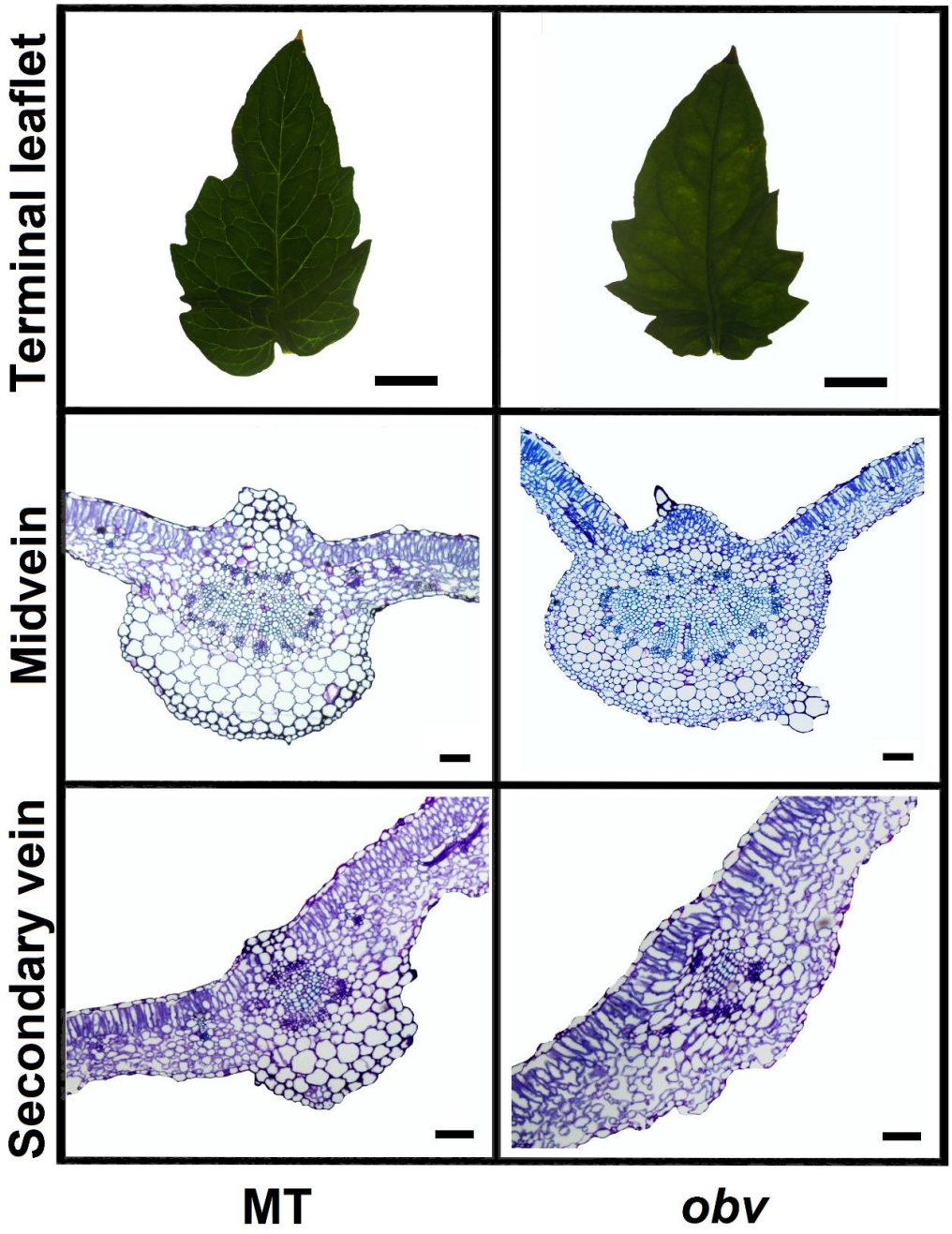

Figure S2. Representative terminal leaflets of Micro-Tom (MT) and the *obscuravenosa* (*obv*) mutant. Cross-sections of the leaf lamina at the midrib and a secondary vein show the presence (MT) and absence (*obv*) of bundle sheath extensions (BSEs). The BSEs have a columnar nature toward the adaxial epidermis, with thickened cells walls, whereas they thicken downward and are broadly based upon the lower epidermis. In the case of *obv*, the continuity of the palisade mesophyll on the adaxial side, and of the spongy mesophyll on the abaxial side, is not interrupted by the cells of the bundle sheath. Scale bars= 1 cm (leaflets) and 100 µm (middle vein and secondary vein).

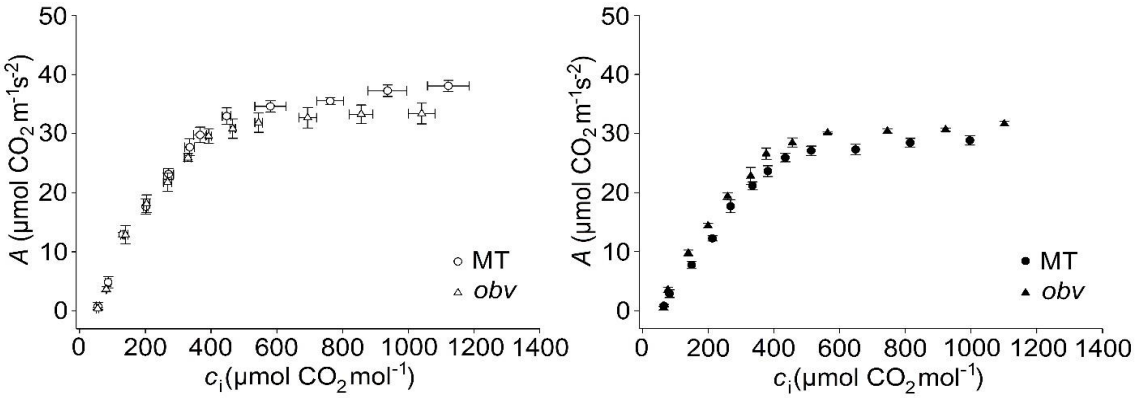

Figure S3. Photosynthetic assimilation rate (*A*) in response to the intercellular CO_2 mole fraction, for Micro-Tom (MT) and the *obscuravenosa* (*obv*) mutant plants grown in the sun (left) or shade (right). Points are means and error bars are s.e.m. (n=4).

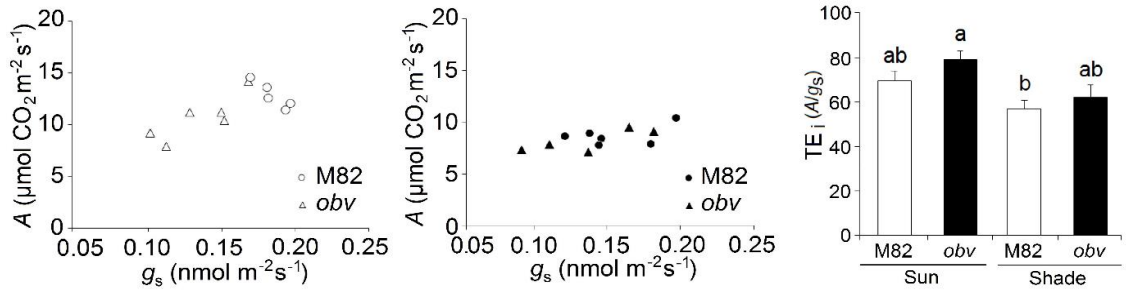

Figure S4. Relationship between photosynthetic CO_2 assimilation rate (*A*) and stomatal conductance (g_s) for M82 (heterobaric) and the *obscuravenosa* (*obv*, homobaric) mutant plants grown in the sun (left) or shade (right). Each point corresponds to an individual measurement. Intrinsic transpiration efficiency (TE_i), calculated from the dataset on the left. Bars are mean values ± s.e.m. (n=5). Different letters indicate significant differences by Tukey's test at 5% probability.

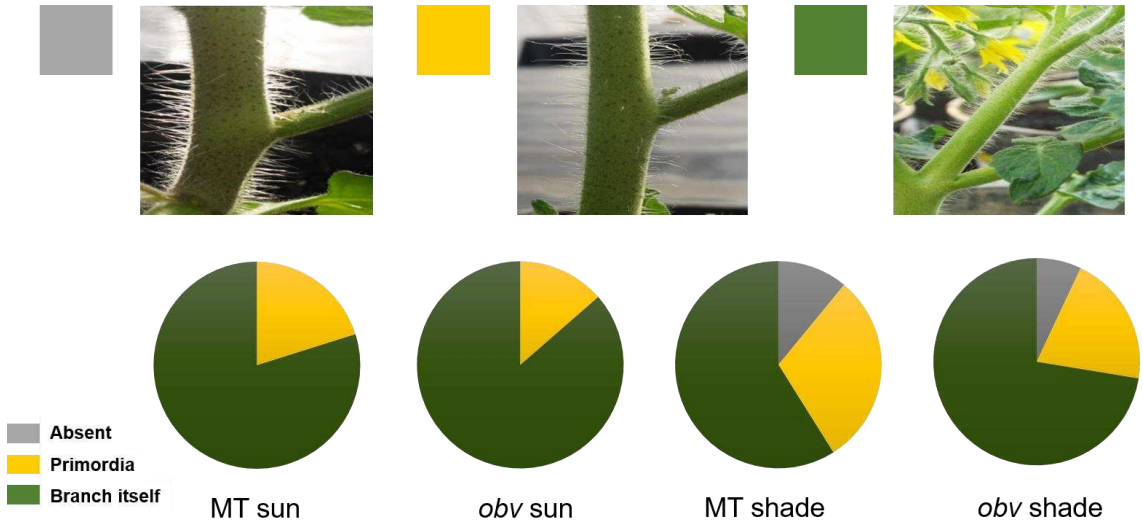

Figure S5. Branching pattern in tomato Micro-Tom (MT) and mutant *obv* in two irradiance levels (sun/shade, 900/300 µmol photons m^{-2} s^{-1}). Branching was determined visually in 45-day-old plants (n=6). The pie charts show the proportion of leaves with no visible primordium (grey), visible primordium (yellow) or fully-developed branch (green) in the axil.

Literature cited

Abramoff MD, Magalhães PJ, Ram SJ (2004) Biophotonics international. Biophotonics Int **11**: 36–42

Assmann SM (1999) The cellular basis of guard cell sensing of rising CO2. Plant Cell Environ **22**: 629–637

Bolaños JA, Hsiao TC (1991) Photosynthetic and respiratory characterization of field grown tomato. Photosynth Res **28**: 21–32

Bonhomme V, Picq S, Gaucherel C, Claude J, Bonhomme V, Picq S, Gaucherel C, Claude J (2014) Momocs: Outline Analysis Using R. J Stat Softw **56**: 1–24

Brodribb TJ (2009) Xylem hydraulic physiology: The functional backbone of terrestrial plant productivity. Plant Sci **177**: 245–251

Buckley TN, John GP, Scoffoni C, Sack L (2015) How does leaf anatomy influence water transport outside the xylem? Plant Physiol **168**: 1616–35

Buckley TN, Sack L, Farquhar GD (2016) Optimal plant water economy. Plant Cell Environ **40**: 1–16

Buckley TN, Sack L, Gilbert ME (2011) The role of bundle sheath extensions and life form in stomatal responses to leaf water status. Plant Physiol **156**: 962–973

Campos ML, Carvalho RF, Benedito VA, Peres LEP (2010) Small and remarkable. The Micro-Tom model system as a tool to discover novel hormonal functions and interactions. Plant Signal Behav **5**: 1–4

Carmo-Silva E, Scales JC, Madgwick PJ, Parry MAJ (2015) Optimizing Rubisco and its regulation for greater resource use efficiency. Plant Cell Environ **38**: 1817–1832

Carvalho RF, Campos ML, Pino LE, Crestana SL, Zsögön A, Lima JE,

Benedito VA, Peres LE (2011) Convergence of developmental mutants into a single tomato model system: "Micro-Tom" as an effective toolkit for plant development research. Plant Methods **7**: 18

Chitwood DH, Kumar R, Ranjan A, Pelletier JM, Townsley BT, Ichihashi Y, Martinez CC, Zumstein K, Harada JJ, Maloof JN, e outros (2015) Light-induced indeterminacy alters shade-avoiding tomato leaf morphology. Plant Physiol **169**: 2030–2047

Cochard H, Venisse J-S, Barigah TS, Brunel N, Herbette S, Guilliot A, Tyree MT, Sakr S (2007) Putative role of aquaporins in variable hydraulic conductance of leaves in response to light. Plant Physiol **143**: 122–133

Esau K (1977) Anatomy of seed plants, 2nd ed. John Wiley & Sons, Inc., New York

Evans JR, vonCaemmerer S (1996) Carbon dioxide diffusion inside leaves. Plant Physiol **110**: 339–346

Farquhar GD, von Caemmerer S, Berry JA (1980) A biochemical model of photosynthetic CO2 assimilation in leaves of C3 species. Planta **149**: 78–90

Fernie AR, Roscher A, Ratcliffe RG, Kruger NJ (2001) Fructose 2,6-bisphosphate activates pyrophosphate: Fructose-6-phosphate 1-phosphotransferase and increases triose phosphate to hexose phosphate cycling heterotrophic cells. Planta **212**: 250–263

Flexas J, Niinemets Ü, Gallé A, Barbour MM, Centritto M, Diaz-Espejo A, Douthe C, Galmés J, Ribas-Carbo M, Rodriguez PL, e outros (2013) Diffusional conductances to CO_2 as a target for increasing photosynthesis and photosynthetic water-use efficiency. Photosynth Res **117**: 45–59

Gay AP, Hurd RG (1975) Influence of light on stomatal density in tomato. New Phytol **75**: 37–46

Genty B, Briantais J-M, Baker NR (1989) The relationship between the quantum yield of photosynthetic electron transport and quenching of chlorophyll fluorescence. Biochim Biophys Acta **990**: 87–92

Guyot G, Scoffoni C, Sack L (2012) Combined impacts of irradiance and dehydration on leaf hydraulic conductance: Insights into vulnerability and stomatal control. Plant, Cell Environ **35**: 857–871

Hacker J, Neuner G (2007) Ice propagation in plants visualized at the tissue level by infrared differential thermal analysis (IDTA). Tree Physiol **27**: 1661–1670

Iwata H, Niikura S, Matsuura S, Takano Y, Ukai Y (1998) Evaluation of variation of root shape of Japanese radish (*Raphanus sativus* L.) based on image analysis using elliptic Fourier descriptors. Euphytica **102**: 143–149

Iwata H, Ukai Y (2002) SHAPE: A computer program package for quantitative evaluation of biological shapes based on elliptic fourier descriptors. J Hered **93**: 384–385

Jones CM, Rick CM, Adams D, Jernstedt J, Chetelat RT (2007b) Genealogy and fine mapping of *obscuravenosa*, a gene affecting the distribution of chloroplasts in leaf veins, and evidence of selection during breeding of tomatoes (*Lycopersicon esculentum*; Solanaceae). Am J Bot **94**: 935–947

Karabourniotis G, Bornman JF, Nikolopoulos D (2000) A possible optical role of the bundle sheath extensions of the heterobaric leaves of *Vitis vinifera* and *Quercus coccifera*. Plant, Cell Environ **23**: 423–430

Kenzo T, Ichie T, Watanabe Y, Hiromi T (2007) Ecological distribution of homobaric and heterobaric leaves in tree species of Malaysian lowland tropical rainforest. Am J Bot **94**: 764–775

Lawson T, Morison J (2006) Visualising patterns of CO_2 diffusion in leaves. New Phytol **169**: 641–3

Leegood RC (2008) Roles of the bundle sheath cells in leaves of C3 plants. J Exp Bot **59**: 1663–1673

Lloyd J, Bloomfield K, Domingues TF, Farquhar GD (2013) Photosynthetically relevant foliar traits correlating better on a mass vs an area basis: of ecophysiological relevance or just a case of mathematical imperatives and statistical quicksand? New Phytol **199**: 311–21

Marti E, Gisbert C, Bishop GJ, Dixon MS, Garcia-Martinez JL (2006) Genetic and physiological characterization of tomato cv. Micro-Tom. J Exp Bot **57**: 2037–2047

Maxwell K, Johnson GN (2000) Chlorophyll fluorescence - a practical guide. J Exp Bot **51**: 659–668

Mott KA (2007) Leaf hydraulic conductivity and stomatal responses to humidity in amphistomatous leaves. Plant Cell Environ **30**: 1444–1449

Mott KA, Gibson AC, Oleary JW (1982) The adaptive significance of amphistomatic leaves. Plant Cell Environ **5**: 455–460

Mott K, Peak D (2010) Stomatal responses to humidity and temperature in darkness. Plant Cell Environ **33**: 1084–1090

Nicotra AB, Cosgrove MJ, Cowling A, Schlichting CD, Jones CS (2008) Leaf shape linked to photosynthetic rates and temperature optima in South African Pelargonium species. Oecologia **154**: 625–35

Nicotra AB, Leigh A, Boyce CK, Jones CS, Niklas KJ, Royer DL, Tsukaya H (2011) The evolution and functional significance of leaf shape in the angiosperms. Funct Plant Biol **38**: 535–552

Niinemets Ü, Cescatti A, Rodeghiero M, Tosens T (2006) Complex adjustments of photosynthetic potentials and internal diffusion conductance to current and

previous light availabilities and leaf age in Mediterranean evergreen species Quercus ilex. Plant, Cell Environ **29**: 1159–1178

Niklas KJ (1992) Plant biomechanics: an engineering approach to plant form and function. University of Chicago Press

Nikolopoulos D, Liakopoulos G, Drossopoulos I, Karabourniotis G (2002) The relationship between anatomy and photosynthetic performance of heterobaric leaves. Plant Physiol **129:** 235-243

Oguchi R, Hikosaka K, Hirose T (2003) Does the photosynthetic light-acclimation need change in leaf anatomy? Plant Cell Environ **26**: 505–512

Oguchi R, Hikosaka K, Hirose T (2005) Leaf anatomy as a constraint for photosynthetic acclimation: differential responses in leaf anatomy to increasing growth irradiance among three deciduous trees. Plant Cell Environ **28**: 916–927

Oguchi R, Hikosaka K, Hiura T, Hirose T (2006) Leaf anatomy and light acclimation in woody seedlings after gap formation in a cool-temperate deciduous forest. Oecologia **149**: 571–582

Pieruschka R, Schurr U, Jensen M, Wolff WF, Jahnke S (2006) Lateral diffusion of CO_2 from shaded to illuminated leaf parts affects photosynthesis inside homobaric leaves. New Phytol **169**: 779–788

Read J, Stokes A (2006) Plant biomechanics in an ecological context. Am J Bot **93**: 1546–1565

Rodeghiero M, Niinemets Ü, Cescatti A (2007) Major diffusion leaks of clamp-on leaf cuvettes still unaccounted: How erroneous are the estimates of Farquhar et al. model parameters? Plant, Cell Environ **30**: 1006–1022

Sack L, Cowan PD, Jaikumar N, Holbrook NM (2003) The “hydrology” of leaves: co-ordination of structure and function in temperate woody species. Plant,

Cell Environ **26**: 1343–1356

Sack L, Holbrook NM (2006) Leaf hydraulics. Annu Rev Plant Biol **57**: 361–381

Sack L, Scoffoni C (2013) Leaf venation: structure, function, development, evolution, ecology and applications in the past, present and future. New Phytol **198**: 983–1000

Sack L, Scoffoni C, McKown AD, Frole K, Rawls M, Havran JC, Tran H, Tran T (2012) Developmentally based scaling of leaf venation architecture explains global ecological patterns. Nat Commun **3**: 837

Scoffoni C, Kunkle J, Pasquet-Kok J, Vuong C, Patel AJ, Montgomery RA, Givnish TJ, Sack L (2015) Light-induced plasticity in leaf hydraulics, venation, anatomy, and gas exchange in ecologically diverse Hawaiian lobeliads. New Phytol **207**: 43–58

Scoffoni C, Pou A, Aasamaa K, Sack L (2008b) The rapid light response of leaf hydraulic conductance: New evidence from two experimental methods. Plant, Cell Environ **31**: 1803–1812

Shimazaki K, Doi M, Assmann SM, Kinoshita T (2007) Light regulation of stomatal movement. Annu Rev Plant Biol **58**: 219–247

Terashima I (1992a) Anatomy of nonuniform leaf photosynthesis. Photosynth Res **31**: 195–212

Terashima I, Miyazawa SI, Hanba YT (2001) Why are sun leaves thicker than shade leaves? Consideration based on analyses of CO_2 diffusion in the leaf. J Plant Res **114**: 93–105

Valentini R, Epron D, Angelis PDE, Matteucci G, Dreyer E (1995) In situ estimation of net CO_2 assimilation, photosynthetic electron flow and photorespiration in Turkey oak (*Q. cerris* L.) leaves: diurnal cycles under different

levels of water supply. Plant Cell Environ **18**: 631–640

Wellburn AR (1994) The spectral determination of chlorophylls a and b, as well as total carotenoids, using various solvents with spectrophotometers of different resolution. J Plant Physiol **144**: 307–313

Wickham H (2016) ggplot2: elegant graphics for data analysis, 2nd ed. Springer

Wylie RB (1952) The bundle sheath extension in leaves of dicotyledons. Am J Bot **39**: 645–651

Zsögön A, Alves Negrini AC, Peres LEP, Nguyen HT, Ball MC (2015) A mutation that eliminates bundle sheath extensions reduces leaf hydraulic conductance, stomatal conductance and assimilation rates in tomato (*Solanum lycopersicum*). New Phytol **205**: 618–626

Zwieniecki MA, Brodribb TJ, Holbrook NM (2007) Hydraulic design of leaves : insights from rehydration kinetics. Plant, Cell Environ 30: 910–921

CHAPTER II

The *obscuravenosa* mutation mitigates the effects of soil water deficit in tomato

Authors: Maria Antonia M. Barbosa[1]; Mateus H. Vicente[2]; Lázaro E. P. Peres[2]; Dimas Mendes Ribeiro[1]; Wagner L. Araújo[1,3]; Agustin Zsögön[1*]

Affiliations

[1]*Departamento de Biologia Vegetal, Universidade Federal de Viçosa, CEP 36570-900, Viçosa, MG, Brazil*

[2]*Laboratory of Hormonal Control of Plant Development. Departamento de Ciências Biológicas, Escola Superior de Agricultura "Luiz de Queiroz", Universidade de São Paulo, CP 09, 13418-900, Piracicaba, SP, Brazil*

[3]*Max-Planck Partner group at the Departamento de Biologia Vegetal, Universidade Federal de Viçosa, 36570-900, Viçosa, MG, Brazil.*

Key words: water deficit, leaf water potential, *obscuravenosa*, *Solanum lycopersicum*

Abstract

Leaves constantly face imbalances between water supply and transpiration rates, a fact that is also associated with their internal hydraulic environment. Heterobaric leaves present an efficient transport of water to the epidermis, due to a better hydraulic integration of the leaf, also presenting a lower resistance to water transport. On the other hand, homobaric leaves are less hydraulically integrated and have a higher resistance to water movement. Tomato leaves (*Solanum lycopersicum* L.) are classified as heterobaric, however, the *obscuravenosa* (*obv*) mutation, which is found in many commercial tomato varieties, has homobaric leaves. We examined the consequences of soil water deficit on the function of heterobaric (MT) and

homobaric (*obv*) leaves of tomato plants. We show that *obv* mutants maintained higher leaf water potential values (Ψ_{leaf}) compared to WT and reduced leaf lamina rolling during eight days of water deficit. We further assessed stomatal responses in WT and *obv* leaves and show that ABA does not trigger stomatal closure in the homobaric mutant. Our results suggest that the *obv* mutation confers a hydraulic advantage for tomato plants under water scarcity, probably via an ABA-independent mechanism.

Introduction

Leaves are the evolutionary solution to the problems of light capture and gas exchange, which have been central drivers of plant evolution since their transition from the aquatic to the terrestrial environment around 450 Mya (Nicotra et al., 2011; Niklas, 2016). The relationship between leaf structure and function is thus fundamental for plant ecological and agricultural performance. Of particular relevance is the role of leaves in the soil-plant-atmosphere hydraulic continuum (Sack & Holbrook, 2006). The reason behind this is that leaves represent a hydraulic bottleneck and therefore a hub were multiple endogenous and exogenous signals are integrated and relayed.

Plants maintain a stable leaf water potential (Ψ_w) through regulation of the fine balance between water supply from the soil and demand from the atmosphere. Supply can be optimized structurally by biochemically enchancing water flow (*e.g.* aquaporins) and/or by more efficient 'piping' (*i.e.* venation pattern and distribution). Both the role of aquaporins (Chaumont & Tyerman, 2014; Maurel et al., 2016) and of leaf venation (Sack & Scoffoni, 2013) in plant function have been aptly reviewed recently. Some of the key parameters influencing the performance of leaf veins are caliber, density and interconnectedness (Sack e Scoffoni, 2013). Subsidiary structures associated with leaf veins also contribute to their function, among them, the bundle sheath (Leegood, 2008) and the bundle sheath extensions (Buckley et al., 2011).

Bundle sheath extensions (BSEs) are vertical rows of colorless cells protruding from veins of different caliber to either or both the adaxial and abaxial epidermis (Wylie, 1952). BSEs may thus cause a 'chambering' of the leaf blade by limiting lateral gas flow (Terashima, 1992). Partial pressure of CO_2 can vary independently between compartments in the blade, thus producing 'heterobaric' leaves (Neger, 1918). In contrast, BSEs are absent in 'homobaric' leaves, wherein homogeneous CO_2 levels are produced through unimpeded lateral gas diffusion. Large-scale surveys have shown a differential distribution of species with homobaric and heterobaric leaves (McClendon, 1992; Kenzo et al., 2007). Homobaric species tend to be more prevalent in the understory, whereas heterobaric ones are more common in the canopy of climax forests. Also, evergreen trees tend to be homobaric whereas deciduous tree species are more frequently heterobaric. This markedly skewed distribution of homobaric and heterobaric species implies some important ecological role for BSEs in response to light intensity and vapor pressure deficit. Lack of BSEs, for instance, could be adaptive in shaded environments, where free lateral CO_2 diffusion could enhance utilization of sunflecks to drive photosynthesis (Lawson & Morison, 2006; Pieruschka et al., 2006).

Multiple hypothetical roles have been ascribed to BSEs in plants, some of which have been confirmed experimentally. They could provide mechanical support (Read & Stokes, 2006), prevent the spread of disease (Lawson & Morison, 2006) and ice (Hacker e Neuner, 2007) in the leaf lamina. A function as enhancers of light distribution within the leaf blade has been demonstrated (Karabourniotis et al., 2000; Nikolopoulos et al., 2002). This is due to their transparency, which causes light refraction and therefore improves photosynthetic rates of thicker leaves. Perhaps most importantly, BSEs appear to function as a pathway for the flow of liquid water between the vascular bundle and the epidermis (Armacost, 1944; Zwieniecki et al., 2007; Buckley et al., 2011). This could provide a means to convey information on the plant's water status directly to the stomata, whose opening and closure regulates transpiratory water loss (Buckley, 2005).

We have previously characterized a tomato mutant (*Solanum lycopersicum* L.) that lacks BSEs (Zsögön et al., 2015). The *obscuravenosa* (*obv*) mutant reduces K_{leaf} and stomatal conductance, albeit with no penalty on biomass production. Here, we tested whether the presence of BSEs could have an impact on plant function in response to soil water deficit. Based on existing physiological information and on the ecological distribution of species with and without BSEs, we hypothesized that plants possessing BSEs would perform better under soil water deficit than plants without BSEs. We cultivated plants of tomato cultivar Micro-Tom (MT) and its near-isogenic *obv* mutant in single pots and determined key water relation parameters over the course of a water withdrawal treatment. We discuss the potential role of BSEs in responding to water deficit.

Material and Methods

Plant material

Seeds of the tomato (*Solanum lycopersicum* L.) cv Micro-Tom (MT) and cv M82 were kindly donated by Dr Avram Levy (Weizmann Institute of Science, Israel) and Dr Roger Chetelat (Tomato Genetics Resource Center, Davis, University of California, CA, USA), respectively. The introgression of the *obscuravenosa* (*obv*) into the MT genetic background was described previously (Carvalho et al., 2011) (Table S1).

Growth conditions

Data were obtained from two independent assays. Plants were grown in a greenhouse in Viçosa (642 m asl, 20º 45' S; 42º 51' W), Minas Gerais, Brazil, under semi-controlled conditions. Plants of tomato cv Micro-Tom (MT) and cv M82 were grown during the months of August to October of 2016 in temperature of 24/20°C, 12/12h (day/night) photoperiod, relative humidity of 70/80%, and radiation of 850-950 µmol m^{-2} s^{-1}. Seeds were sterilized in hypochlorite sodium solution 30% for 30

min, and subsequent washes with deionized water. Sowing was carried out under greenhouse conditions. The seeds were sown in polyethylene trays containing commercial substrate of Tropostrato® and germination occurred about seven days after sowing. The transplantio was carried out with seedlings that had two completely expanded lines using polyethylene pots, with a capacity of 0.3 and 3.5L for MT and M82, respctively, containing the same type of substrate used for sowing fertilized with 8g of NPK formulation 4:14:8 and 4g of limestone per liter. In addition, weekly foliar fertilization was carried out using Biofert® leaf fertilizer 6-4-14 (Biokits, Contagem, MG, Brazil) at a concentration of 2g per liter, and fertilizations every 15 days, using 0.5 g of NPK formulation 4:14:8.

Experimental setup

The study was conducted in completely randomized experimental design, using two genotypes (MT and *obv*), and two conditions of water regime (well-watered and water deficit). In the experiment 15 pots were used and in each vessel contained two plants (one of each genotype). All plants were irrigated until the age of 30 days. The irrigation was performed daily, twice a day, in a controlled manner, so that each pot received the same volume of water. The irrigation was maintained in 5 pots throughout the experiment and in 10 vessels the irrigation was suspended. The water deficit treatment plants were submitted to 10 days of drought (0 at 9 points). On the 9th day of water deficit, five pots were re-irrigated, consisting of the rehydration treatment.

Leaf water potential (Ψ_{leaf}) and Relative water content (RWC)

The leaf water potential (Ψ_{leaf}) measurements were performed at five points during the water deficit (days 0, 2, 5, 7 and 8) and on the 9th day after the rehydration was applied. The data were obtained using a Scholander-type pressure chamber (model 1000, PMS Instruments, Albany, NY, USA). Measurements were performed from 12:00 to 14:00, with temperature was 25.5° C and the relative

humidity ranged between 60 and 80% throughout the day. The Ψ_{leaf} was always evaluated in the central leaflet of the expanded leaf.

The Relative Water Content (RWC) was determined without day 0 and 8 of water deficit, using the side leaflet of the 4th and 5th fully expanded leaf. The leaflets were weighed and the weight fresh (FW). Subsequently, they were submerged in distilled water and kept under laboratory conditions at a temperature of 24° C and relative humidity of about 60%. After 24 hours, the leaflets were weighed and obtained at turgid weight (TW), and dried at 70° C for 48 hours and reweighed to dry weight (DW). The samples were then weighed in a semi-analytical balance (Shimadzu®, AUY220 model, Kyoto, Japan) with a sensitivity of 0.01 g. RWC was determined using formula:

$$RWC = [(FW - DW)/(TW - DW)] \times 100$$

Water loss of soil and plant phenotypes

The water loss of soil, leaf roll rate parameters and observations of the plants were evaluated every day of water deficit. The loss of soil water was evaluated by means of weighing of the pots in digital balance electronic scale (Toledo®, model 9094, São Paulo, Brazil). The vessels under well-watered treatment were irrigated every day until reaching the vessel's field capacity. The wilting symptoms of the plants was obtained through visual analysis and the images were recorded with a digital camera (FUJIFILM® model FinePix S8200, Tokyo, Japan). Leaf roll rate was evaluated during all treatment days in the median region of the central leaflet of the fully expanded 5th leaf that was previously marked. Measurements were made using a mechanical pachymeter (Mitutoyo® Vernie Caliper model, Japan). The leaf roll was observed every day during the water deficit period and recorded with a digital camera (FUJIFILM® model FinePix S8200, Tokyo, Japan). After rehydration, evaluate the leaf roll rate, for four consecutive hours, based on the same leaflet used previously. The leaflet phenotype was recorded simultaneously.

Kinetics of stomatal conductance

The evaluation of the stomatal behavior in response to variation in light intensity and leaf water supply, was performed in an independent assay in MT and *obv* plants in Micro-Tom *background*. The evaluations were made in plants with age of 45 dag, under laboratory conditions (temperature 22-25°C; relative humidity 50-60% and radiation of 150-200 µmol m^{-2} s^{-1}), using open-flow gas exchange system infrared gas analyzer (IRGA) model LI-6400XT (Li-Cor, Lincoln, NE, USA). The variation of stomatal conductance (g_s) on detached leaves was observed after the detachment of the fully expanded fifth or sixth central leaflet. After the stabilization of the g_s, the apparatus was programmed to read every 30 sec and the leaflet was detached from the plant. The self-reading program was maintained until a new stabilization of the g_s. At the end of this evaluation the relative variation of g_s was calculated. For this purpose, the value of g_s registered at the time of the secondment was used. The parameters of WWR -wrong-way responses (absolute size, WWR length and WWR rate opening) were calculed according by Buckley et al. (2011). The kinetics of g_s and rate of assimilation (A) in response to light variation, were performed under the same conditions described above, however, the leaflets were not detached from the plant. The readings were performed every 20 sec after the stabilization of the gs values. The first reading was performed in a 10 min interval with a 100 µmol m^{-2} s^{-1}, then the radiation was increased to 1000 µmol m^{-2} s^{-1}, where a reading followed for another 15 min under this intensity. Subsequently, the radiation was returned to the initial value (100 µmol m^{-2} s^{-1}) and remained under evaluation for another 10 min. The alternation in the amount of light was based on the results presented by Lawson et al. (2010).

Measurement of water loss

For both genotypes (MT and M82) the water loss was evaluated using the leaflet of the fully expanded fifth leaf in plants with age of 40 and 50 days,

respectively. Leaflets were floated in 10 mM MES-KOH buffer, pH 6.15, 5 mM KCl, and 50 mM $CaCl_2$ at 25° C, for 2.5 h, under light conditions (60-100 µE m^{-2} s^{-1}) in a growth chamber. Following this, leaflets were treated with ABA (50 µM) and incubed in the same buffer medium for a further 2.5 h. Water loss of detached leaflets was measured by weighing leaflets placed abaxial side up on open Petri dishes (30 mm diameter) with one layer of filter paper (Whatman number 1), under a direct light source (50 cm from a 60 Watt bulb), on the laboratory bench. The weight of each set of leaflet was determined every 15 min over a period of 4 h. Water loss was expressed as the percentage of the initial weight.

Stomatal analysis

The stomatal opening evaluation was performed under treatment of ABA in two concentrations levels (5 µM and 50 µM). Leaflets were floated in 10 mM MES-KOH buffer, pH 6.15, 5 mM KCl, and 50 mM $CaCl_2$ at 25° C, and after, treated with ABA and incubed in the same buffer medium for a further 2.5 h (incubation as described for water loss). After the incubation period, dental resin imprints were taken from the abaxial surface of four leaflets, the third and fourth fully expanded leaf (Kagan et al., 1992; Berger & Altmann, 2000). Nail polish copies were prepared as described by Von Groll et al. (2002), and the images were taken with light microscope (Zeiss, Axioscope A1 model, Thornwood, NY, USA) with attached Axiovision® 105 color image capture system, and were evaluated in the Image Pro-Plus® software (version 4.5, Media Cybernetics, Silver Spring, USA). Stomatal aperture measurements were determined in 100 guard cell pairs distributed in at least fifteen separate.

Statistical analyses

The experiment was conducted in a completely randomized experimental design. The data were submitted to analysis of variance (ANOVA) using the

program Assistat version 7.7 (disponible in: http://assistat.com) and the averages were compared by *t* test at the 5% level of significance ($P \leq 0.05$).

Results and discussion

Wilting attenuation in the obscuravenosa (obv) mutant upon water withdrawal

We grew heterobaric cultivar Micro-Tom (MT) tomato plants and the homobaric near-isogenic line harboring the *obscuravenosa* (*obv*) mutation paired in single pots. This is a way to ensure a comparable water supply for both genotypes, as they experience the same soil water potential at all times (Bolaños et al., 1993). The volume of the pots (300 ml) is small enough to prevent the development of large heterogeneities in water content. We suspended watering and scored wilting using a visual scale and concomitantly determined soil water content gravimetrically and midday leaf water potential (Ψ_{leaf}) using a pressure bomb. MT plants wilted faster and in greater proportion than *obv* mutant over the course of the drought treatment (Figures 1A-D).

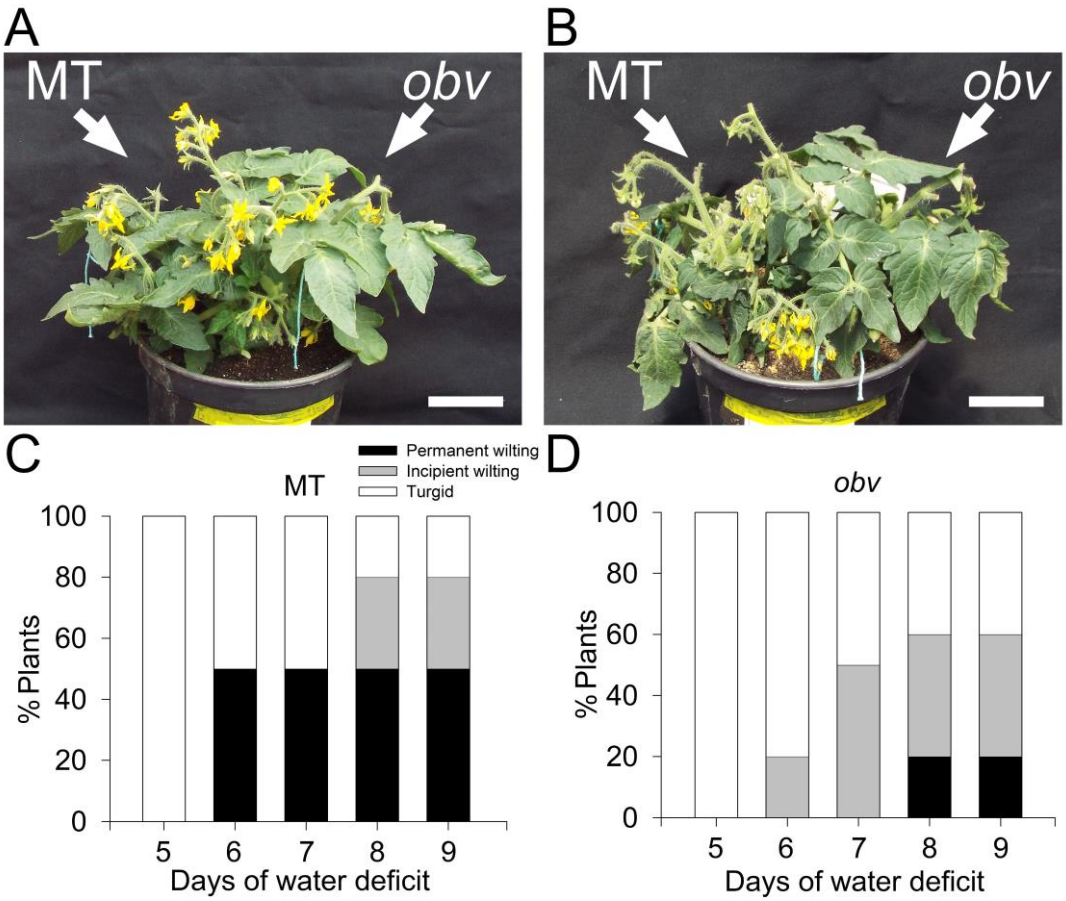

Figure 1. Representative heterobaric (MT) and homobaric (*obv*) tomato plants under two soil hydration levels (control and water deficit). In all photos, MT (left) and *obv* (right). The images are representative for day 0 and day 8 of water deficit. Note that MT has wilting symptoms before *obv*. Bars = 10 cm. Bottom panels show the wilting rate of the each genotype classified in three groups scored visually: turgid, incipient wilting and permanent wilting.

Ψ_{leaf} of the *obv* mutant during eight days of drought was consistently higher in relation to MT plants, with values of -1.0 MPa and -1.4 MPa respectively, on the last day of drought (Figure 2A). Thus, homobaric *obv* plants maintained Ψ_{leaf} 22.8% higher than heterobaric MT plants after 8 days of water deficit (P= 0.02). Higher values of Ψ_{leaf} for *obv* mutant were observed on every day of the experiment, from day five of water withdrawal onward, when stress became more severe (Figure 2A). To confirm the water status of the plants, we also evaluated, the relative water content in leaves (RWC) at the end of the experiment (Figure 2B). RWC did not

differ between MT and the *obv* mutant in the well-watered control treatment (*P*=0.14). At the end of the drought treatment, however, MT plants had significantly lower RWC than well-watered MT plants (*P*=0.0002). Mutant *obv* plants, on the other hand, maintained a similar RWC in both conditions. Soil water loss was monitored daily gravimetrically (Figure 2C). On the eighth day of water withdrawal, pots in the 'drought' treatment had lost 42.4% of their water content in relation to the amount of water at the beginning of the treatment (day 0). Water replenishment on the ninth day of treatment promoted a hydration of 71.6% in the soil, reducing the effects of drought on the plants. Thus, contrary to our first hypothesis, homobaric *obv* tomato plants coped better with soil water deficit than heterobaric ones. A brief deviation about this genotype is in order to provide a better context for the discussion.

In tomato, a library of 76 introgression lines (ILs), each containing an overlapping chromosomal segment from the wild relative *Solanum pennellii* has been instrumental for mapping and cloning of genes controlling traits of interest (Eshed & Zamir, 1994). Interestingly, M82, the tomato background used to create the ILs, is a mutant for *obv*, and thus lacks BSEs. Screening the IL population for $\Delta^{13}C$ (carbon isotope composition, a proxy for long-term water-use efficiency, WUE, (Farquhar e Richards, 1984; Farquhar et al., 1989)) revealed that one line, IL5-4, had the lowest value of $\Delta^{13}C$ (*i.e.*, the highest WUE) (Xu et al., 2008). IL5-4 harbors the *S. pennellii* allele of the *obv* gene, whose molecular identity remains unknown (Jones et al., 2007). Subsequent, more refined analyses using sub-lines created from IL5-4, either with or without BSEs, confirmed the detrimental effect of *obv* on $\Delta^{13}C$ and WUE (Barrios-Masias et al., 2014). Taken together these results led us to hypothesize that the presence of BSEs would improve drought tolerance, as has been proposed before (Buckley et al., 2011). Other observations, however, suggest a different picture can also be reconciled with our present results.

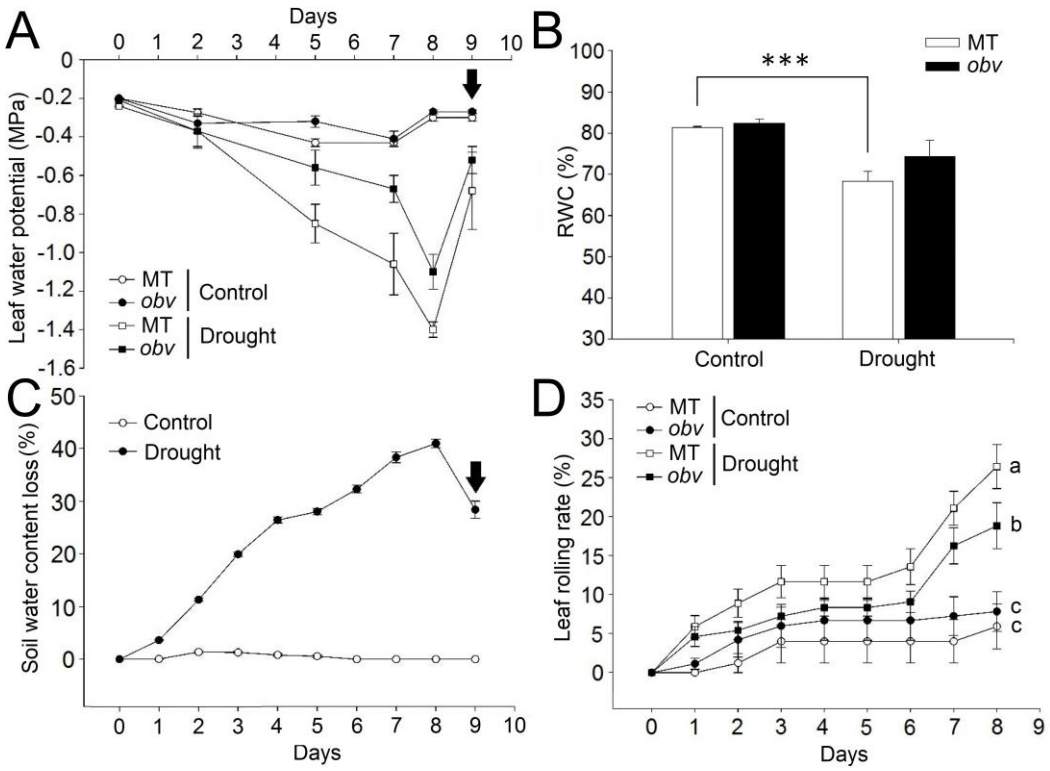

Figure 2. Leaf water potential, relative water content (RWC), water loss of soil and leaf roll rate in tomato plants (cv. Micro-Tom) and *obv* mutant in control and water deficit. The measurements the leaf water potential (A) were always carried out in the range 12:00 to 14:00 h at 0, 2, 5, 7 and 8 days of drought. The arrow indicates the rehydration made at 9 days after the start of drought. (n=5). The RWC measurements (B) were performed after 8 days of dry. The central leaflet 5th fully expanded leaf was detached and immediately weighed, and then the leaflets were placed in petri dishes containing distilled water and weighed after 24 hours of incubation in a direct light source on the laboratory bench. The leaflets were dried in an oven at 70°C for 24 hours. RWC rate was measured according to the formula: RWC (%) = (FW-DW) / (TW-DW) x 100 (n=6). The water loss of soil in pots (C) were weighed during the 10 days of experiment. The pots under control treatment were irrigated every day until the soil reaches its field capacity. The arrow indicates the time of rehydration. Note that there was a reduction in soil water loss. Leaf roll rate in tomatoes plants (cv. Micro-Tom) and *obv* mutant under two hydration levels (WW – well-watered and WD – water deficit). Measurements of leaf roll rate (D) were performed every day of the experiment by measuring the width of the central leaflet of the 5th fully expanded leaf. (n=6). During the experimental period the average temperature was 25.5°C and the relative humidity ranged between 70 and 80% throughout the day.

Firstly, a wider analysis of $\Delta^{13}C$ comparing species with or without BSEs revealed that the relationship between BSEs and WUE differs among species (Lynch

et al., 2012) Secondly, our own previous work showed that g_{max} is lower in the *obv* mutant than in MT (Zsögön et al., 2015). This fits with a recent report showing that plants without BSEs maintain lower g_s and less negative Ψ_{leaf} at midday (Kawai et al., 2017). It has therefore been suggested that plants with BSEs have increased risk of air seeding and cavitation (Zwieniecki et al., 2007; Sommerville et al., 2012). Heterobaric plants thus maintain higher g_s through milder desiccating conditions but are potentially more vulnerable to stronger restrictions in water supply, as illustrated by the reduced hydration level at the end of the water withdrawal treatment in our experiments.

Precise gene annotation of the collection of ILs, revealed that the IL5-4 harbors only 37 genes from *S. pennellii* (Chitwood et al., 2013), thus paving the way for the cloning and characterization of the molecular effects of *OBV*. Further insight into the physiology of homobaric and heterobaric leaves will come when the genetic basis for BSE development is unveiled.

Leaf roll reduction in leaves of the obv mutant lacking BSEs

Leaf roll is a commonly observed response in many crop species, including tomato, which can be either 'physiological' if caused by environmental factors or 'pathological' if the result of a viral infection (Kadioglu et al., 2012). Surprisingly little is known about the genetic and biomechanical basis for this phenomenon, although it can lead to yield and fruit quality losses (Woltz, 1968). Soil water deficit is well-known to induce leaf roll in tomato and other species (Kadioglu e Terzi, 2007). Here, we determined the degree of rolling comparing the width of terminal leaflets over the course of the drought experiment (Figure 2D). At the last day of assessment leaves of both genotypes were significantly more curled in the drought than in their respective control treatment. MT leaves, however, showed a more pronounced (P=0.0318) rolling than *obv* leaves in the drought treatment. This ranking was consistent over the whole course of the assay, however, the differences were more expressive as the water deficit became more severe (Figure 2D).

Rehydration of all the plants was carried out on day nine of water withdrawal and during four consecutive hours, we followed the unwinding of the leaves to compare the response between genotypes. No significant difference was observed in the rate of leaf unrolling (Fig S1).

We have shown here that plants harboring the *obv* mutation display a much reduced leaf roll induced by soil water deficit. This finding suggests that the presence of a bundle sheath extension is a condition for the leaf rolling response in tomato and could explain the observation that susceptibility to this phenomenon varies considerably between cultivars. Indeterminate cultivars are reported to be more sensitive to leaf rolling than determinate ones (Pacific Northwest Extension Group, 2011). A survey of available phenotypic data showed that out of 75 indeterminate tomato cultivars, 67 (89.3%) harbored the *obv* mutation, whereas of 34 determinate cultivars only eight (23.5%) were mutant (Jones et al., 2007). It is therefore reasonable to suggest that the link between the incidence of leaf rolling and tomato growth habit is not causal, but rather linked by a third variable, namely the presence of BSEs, controlled by the *OBV* gene.

Stomatal dynamics are not altered the homobaric obv mutant in response to irradiance and leaf excision

The results described above point to a possible role of stomata in the differential response of the *obv* mutant to soil water deficit. We previously showed that the *obv* mutant maintains lower stomatal conductance in well-watered conditions (Zsögön et al., 2015). Stomata respond dynamically to environmental conditions (Lawson et al., 2010), so here we conducted two assays, one affecting light intensity and the other, water supply to the leaves. We assessed the kinetics of stomatal conductance (g_s) in response to step-changes in irradiance ("sunflecks") (Kirschbaum et al., 1988) or the "wrong-way response" (WWR) in stomatal conductance following leaf excision (Powles et al., 2006).

The stomatal response following dark-to-light and light-to-dark transitions in photosynthetically active photon flux density (PPFD) 100-1000-100 µmol m^{-2} s^{-1}, with a duration of 15 minutes in the high irradiance interval. The initial g_s values were similarly low for both MT and *obv* (0.048 and 0.060 mol m^{-2} s^{-1}, respectively; *P*=0.38). Increase in irradiance intensity led initially to a three-minute lag period, after which g_s increased, reaching a peak of ~0.200 mol m^{-2} s^{-1} after 15 minutes (Figure 3A). Switching the light intensity back to the low level triggered an instantaneous decrease in g_s for both genotypes. The values returned to the starting ones after ten minutes. Assimilation rates increased steadily over the duration of the sunfleck, with similar values for both genotypes and approximately following stomatal opening.

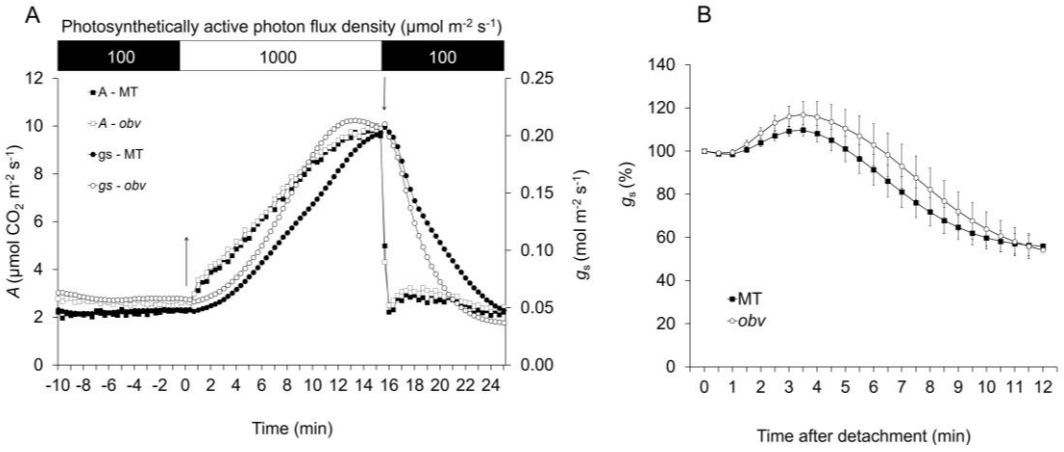

Figure 3. Stomatal aperture and closure kinetics in response to light Micro-Tom (MT) and *obscuravenosa* (*obv*) mutant (A) and rate of decrease of stomatal conductance (gs) in detached leaves compared to gs stabilized at the beginning of the assessment (B). Stomatal conductance (g_s) and assimilation rate (*A*) was evaluated in MT and *obv* in response to changes in light intensity. Measurements were performed using a LI-6400; LI-COR gas exchange chamber. Data presented are mean ± SE obtained using the 5th or 6th leaf totally expanded. (n=6).

The stomatal response to light comprises two components: a photosynthesis-driven one, to red light and a photosynthesis-independent to blue light (Shimazaki et al., 2007). While the blue light response operates quickly and directly at the level of guard cells (Zeiger et al., 1985), the red light response appears to be governed by

mesophyll consumption of CO_2 (Roelfsema et al., 2002). In tobacco, however, no difference was found between the response to either red or red and blue light and stomatal conductance depended solely on the light intensity regardless of quality (Lawson et al., 2010). This suggests that the dynamic response of stomata to fluctuating light conditions is complex and probably species-dependent (Lawson et al., 2010). Of particular interest is the duration of the light stimulus. Stomatal aperture displays complex interaction with assimilation rates in the mesophyll (von Caemmerer et al., 2004). Within the first 10 minutes of light induction assimilation rate is limited biochemically by Rubisco and light-harvesting complex activation (Barradas e Jones, 1996). Afterwards, stomatal aperture can limit assimilation rate. The response to shade flecks (brief periods of low light intensity) is similarly complex. Shade flecks of less than five minutes will not impact g_s considerably, but lower only assimilation rate. Longer shading can trigger stomatal closure, which can 'overshoot' and persist after light has been restored (Kirschbaum et al., 1988). This, in turn can delay the restoration of steady-state assimilation rates for 10-15 minutes. We did not observe significant differences in the response to red and blue light here, but the present study should be refined to allow more solid conclusions.

The WWR is a phenomenon whereby perturbations in the plants hydraulic system lead to transient stomatal responses in opposite direction to the steady-state ones (Darwin, 1898; Cowan, 1972). We assessed the response by detaching leaves clamped into an infrared gas analyser after they had attained stable values of g_s in standard gas exchange conditions (CO_2 concentration of 400 ppm; air flow of 350 umol s^{-1}; leaf temperature of 24°C and PAR of 800 µmol m^{-2} s^{-1}) (Figure 3B, Table 1). The response was similar for all leaves of both genotypes, g_s initially increased after detachment, then decreased to values lower than the original $g_{s.}$ We decomposed the response in terms of magnitude of WWR, duration and stomatal opening rate (Powles et al., 2006). Initial g_s was similar for genotypes, and the absolute and relative size of the WWR was not significantly different between

homobaric and heterobaric leaves (Table 1). Duration of the WWR was not different between genotypes either.

Table 1. Parameters of the "wrong-way response" (WWR) in detached leaves of heterobaric (cv. Micro-Tom, MT) or homobaric (*obscuravenosa*, *obv*) tomato plants.

	MT	**CV (%)**	***obv***	**CV (%)**	***p*-value**
g_x (g_s at excision; mol m^{-2} s^{-1})	0.111 ± 0.018	36	0.104 ± 0.013	28	0.7590
Absolute size of WWR (mol m^{-2} s^{-1})	0.106 ± 0.007	16	0.159 ± 0.030	42	0.1286
W=Relative size of WWR (%)	108.99 ± 21.88	44	175.39 ± 43.95	32	0.1165
L=WWR duration (min)	5.80 ± 0.60	23	7.40 ± 1.02	30	0.2441
V=WWR opening rate (W/L)	18.98 ± 3.20	37	26.41 ± 4.28	36	0.2015

Stomata respond to a multiplicity of endogenous and environmental signal to maintain hydraulic homeostasis of the leaf (Buckley, 2005; Buckley et al., 2016). Stomatal aperture is determined not only by guard cell turgor pressure, but also by turgor pressure of the surrounding epidermal pavement cells. BSEs have been proposed to act as a hydraulic connection between vascular bundles and the epidermis (Zwieniecki et al., 2007; Sommerville et al., 2012). This, in turn would increase integration of stomatal responses to water status of the plant. A survey comparing 20 species, half of them homobaric and half heterobaric, showed that WWRs in response to leaf excision were weaker in the former, but with no difference in duration (Buckley et al., 2011). BSEs could thus help reduce water loss when evaporative demand increases and thus enhance drought tolerance. This is in agreement with the ecological distribution of heterobaric species, which are more prevalent in sunny, dry habitats or in the upper stories of climax forests (Wylie,

1952; Kenzo et al., 2007). Our results show no difference in WWR kinetics between homobaric and heterobaric genotypes. It is therefore likely that in our study, BSEs are not reducing the sensitivity in epidermal turgor to changes in hydraulic supply, which means that hydraulic resistance in the leaf lamina is not altered in the pathway from the vascular bundle to the epidermis. This, however, does not fit to our previously published results (Zsögön et al., 2015) and should therefore be explored more in depth with more experimental data. The large coefficients of variation (Table 1) for WWR parameters suggest that other factors besides the presence or absence of BSEs could have been influencing our measurements.

Apparent stomatal insensitivity to abscisic acid (ABA) in the homobaric obv mutant

Water loss is governed by stomatal aperture, which is directly controlled by the accumulation of the hormone ABA under drought conditions (Blackman e Davies, 1983; Lind et al., 2015). We thus performed a test of water loss from leaves to assess the stomatal responses of homobaric and heterobaric leaves in response to ABA (50 μM). We carried out this experiment in two different tomato cultivars: the dwarf cultivar Micro-Tom (MT) and the commercial cultivar M82 (see Table S1 for details). The kinetics of water loss in leaves clearly shows the effect of ABA on the closure of stomata in MT (Figure 4A). When treated with ABA, the leaves of MT plants showed a considerable reduction in water loss rate in the early phase of the assay, compared to leaves in the control treatment (26% *vs* 31%). Homobaric mutant leaves, on the other hand, showed identical rates of water loss from leaves of the control and ABA treatment, (Figure 4B). The fastest water loss occurred in the first 60 min of evaluation for both genotypes (Figures 4C e 4D). For MT plants, there was a significant difference in the maximum rate of water loss between control and ABA treatment (49% *vs* 28%), for the first 15 min of evaluation (P= 0.005) (Figure 4C). The maximum rate of water loss were initially lower for both control and ABA-treated *obv* plants compared to MT, but at the end of the assay, all leaves have undergone a similar amount of fresh weight reduction (Figure 4D). These results

were consistent for M82 plants (Figure S2), where the fresh weight loss for ABA-treated MT was lower than the leaves without treatment with this hormone. For the *obv* mutant, water loss occurred at as similar rate in both treatments.

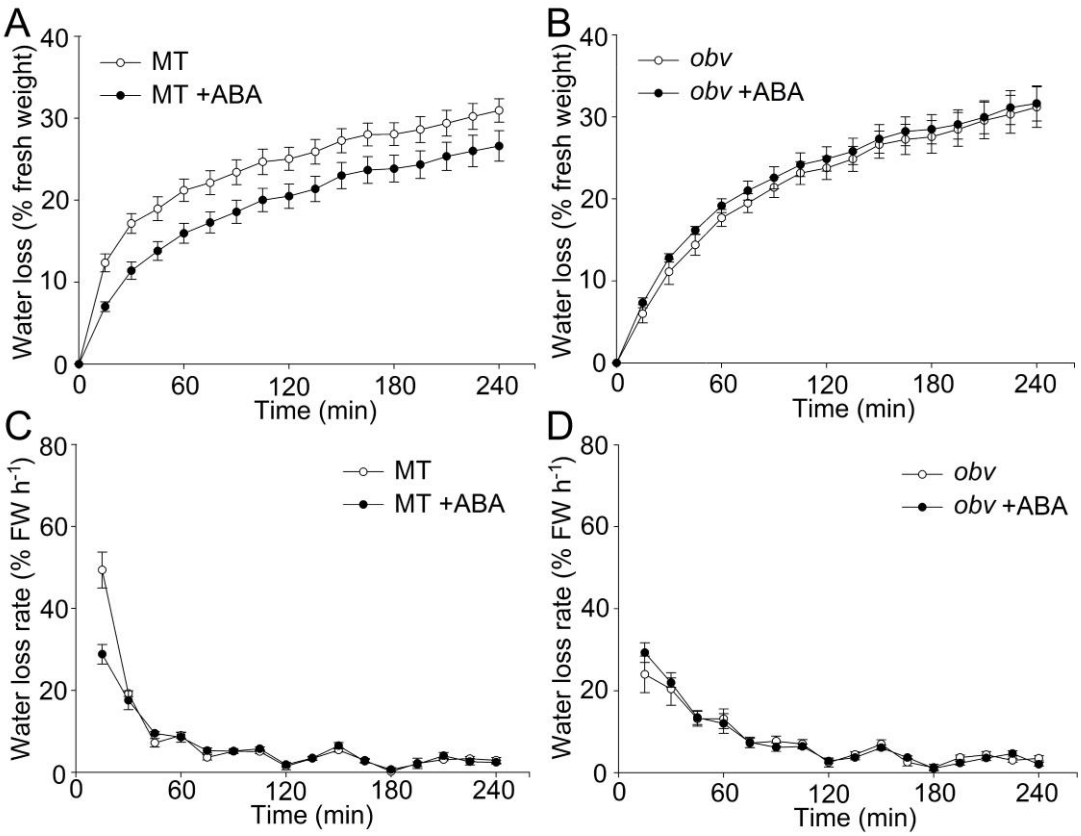

Figure 4. ABA reduces the water loss of MT plants and does not reduce *obv* mutant. Leaves at the same developmental stage and size from 40 DAG plants were floated in MES-KCL buffer under light to induced stomatal apertures (control). Afterwards, leaves were incubated in ABA (50 µM) for 2.5h. The water loss of detached leaves was measured by weighing fresh leaves placed under a direct light source on the laboratory bench. Water loss was expressed as the percentage of initial weight at each time point. Data are averages of five repetitions for each treatment.

Next, we assessed stomatal opening in response to ABA treatments in two level of concentration (5 µM and 50 µM) in excised epidermes of both genotypes. The application of ABA at 5 µM concentration restricted the stomatal opening for both genotypes, compared to the control treatment (Figure 5A), however, the *obv* mutant was less responsive to the exogenous application of this hormone, compared

to MT (*P*= 0.008), showing a stomatal opening 14% larger than MT plants. The same response was observed at the concentration of 50 μM. The *obv* mutant showed an even greater insensitivity to ABA even at a higher concentration of this hormone (*P*= 0.0001) what, stomatal opening of the mutant was similar to the control treatment, however, it was 146% higher compared to MT plants under this concentration (50 μM). The stomatal closure promoted by ABA, induced a reduction in transpiration in MT plants, which was evaluated by the decline of the water loss curve in detached leaves (Figures 4A and C). On the other hand, the movement of guard cells *obv* plants remained unstable under the highest concentration of ABA, corroborating with the similar water loss in leaves detached treated with and without ABA (Figures 4B and D). One of the main mechanisms involved in the regulation of stomatal aperture in soil lack of water is ABA signaling in the guard cells, however, the signaling processes that occur in these cells can be modulated by many stimuli, not yet fully known (Kim et al., 2010). In addition, under drought conditions ABA levels increase in the roots and is perceived by the guard cells, which consequently promotes changes in the ion fluxes leading to the closure of the stomata (Araújo et al., 2011). This behavior does not agree with the possible higher resistance of *obv* plants to drought, as shown in our results. However, the best response of plants without BSE to water deficit may be associated with other mechanisms not yet known, which are probably independent of ABA signaling. The *obv* plants showed insensitivity to the effects of this hormone, regardless of the concentration applied, but interestingly, when a higher concentration of ABA (50 μM) was applied, the response to stomatal closure was even lower when compared to the lowest concentration treatment (5 μM) (Figures 5A and B). It is large difference in mutant response to the two concentrations of ABA, in fact, seems to be an intriguing result, since it is already well known that the increase in ABA concentrations in the guard cells is negatively correlated with stomatal conductance, that is, further promotes the closure of the stomata (Franks & Farquhar, 2001; Ruszala et al., 2011), however, more detailed evaluations of these results need to be made.

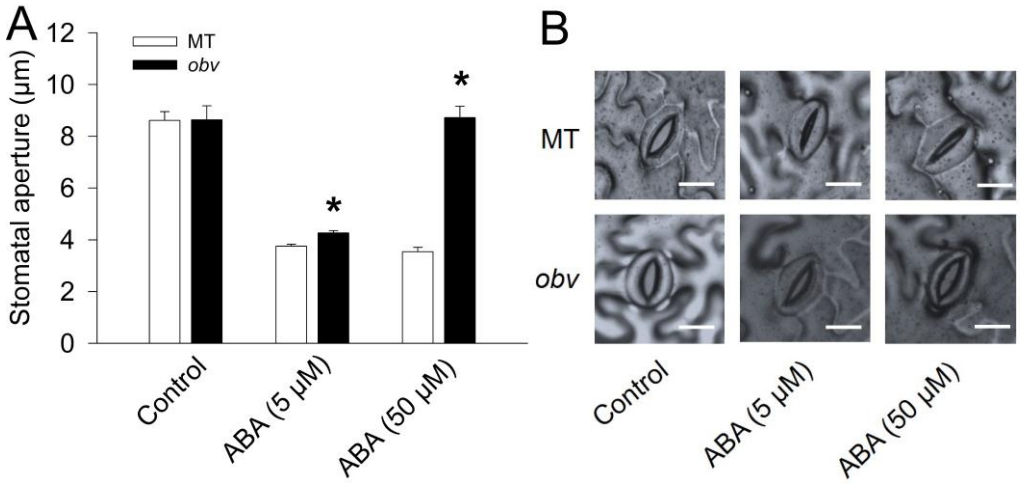

Figure 5. To determine suppression of stomatal closure by ABA, tomato leaflets (Micro-Tom) and mutant *obv* were incubated in stomatal aperture buffer (MES-KCl, pH 6.15) for 2.5 hours and after incubation for same period in ABA 5 µM and 50 µM (A). Fragments of the leaflets were observed under a light microscope to ensure stomatal opening. The images were taken using an optical microscope (B) and the individual stomatal apertures were measured using Image Pro Plus® software. 100 stomata were counted, and a total of four leaflets were used for the analysis of each treatment. The bars represent the mean ± standard error. Asterisks indicate the difference between the two treatments for each genotype according to Tukey test to be significantly different ($P<0.05$). Scale bar = 25 µm.

Conclusions

The absence of BSE positively influenced the response of tomato plants in the condition of low soil water supply. The *obv* mutation that eliminates BSE, contributed to a higher hydration of these plants, which presented higher values of water potential midday, and lower wilting rate. This higher resistance of *obv* plants, however, seems not to be associated with different stomatal responses, which in this work was similar for both genotypes, independently of the level of irradiance and water supply in the leaf. In addition, response *obv* mutant to water deficit does not appear to involve stomatal closure mechanisms in response to ABA. Thus, our results suggest that the *obv* mutation confers a greater hydraulic advantage for tomato plants under water scarcity conditions, and this is probably associated with the structural characteristics of these leaves, which present lower vein density and

greater resistance to water flow (data not shown here). In addition, previous studies have reported that leaves with BSE, presented higher values of g_s and low water potential under water deficit condition, due to osmoregulation mechanisms that maintain the turgor of the guard cells. Finally, we propose that, complementary evaluations of the mechanisms of tolerance promoted by the *obv* mutation in tomato plants, need to be performed to better understand the role of BSE in the hydraulic characteristics of the leaf in tomato plants, since a BSE function in water relations may differ between species.

Acknowledgments

This work was supported by funding from the Agency for the Support and Evaluation of Graduate Education (CAPES-Brazil), the National Council for Scientific and Technological Development (CNPq-Brazil), Foundation for Research Assistance of the São Paulo State (FAPESP-Brazil) and the Foundation for Research Assistance of the Minas Gerais State (FAPEMIG-Brazil). We thank CAPES for studentship granted to M.A.M.B. W.L.A. and L.E.P.P. acknowledge grants from CNPq (grant 307040/2014-3 to L.E.P.P.).

Supplementary information

Tables

Table S1. Description of the plant material used in this study. Micro-Tom (MT) and M82 are two tomato cultivars that differ in growth habit due mostly (but not only, see (Campos et al., 2010) for details) to the presence of a mutant allele of the *DWARF* gene (functional allele capitalized), a brassinosteroid C-6 oxidase, whose product is required for a fully functional brassinosteroid biosynthesis pathway. The molecular identity of *OBSCURAVENOSA* (*OBV*) is unknown. MT harbors a functional, dominant allele of *OBV*, whereas M82 is a mutant, as shown by (Jones et al., 2007). F1 plants are hybrids with a 50/50 MT/M82 genomic complement, differing only in the presence or absence of BSEs. The F1 plants are otherwise phenotypically indistinguishable from the M82 parent. For simplicity, the F1 lines with and without BSEs are referred to as M82 and *obv*.

Parental genotype	MT	MT-*obv*	M82	MT×M82	MT-*obv*×M82
Growth habit					
Genotype	*dwarf/dwarf*	*dwarf/dwarf*	*DWARF/DWARF*	*DWARF/dwarf*	*DWARF/dwarf*
Phenotype	Dwarf plant	Dwarf plant	Tall plant	Tall plant	Tall plant
BSE					
Genotype	*OBV/OBV*	*obv/obv*	*obv/obv*	*OBV/obv*	*obv/obv*
Phenotype	BSEs (clear veins)	No BSEs (dark veins)	No BSEs (dark veins)	BSEs (clear veins)	No BSEs (dark veins)

Figures

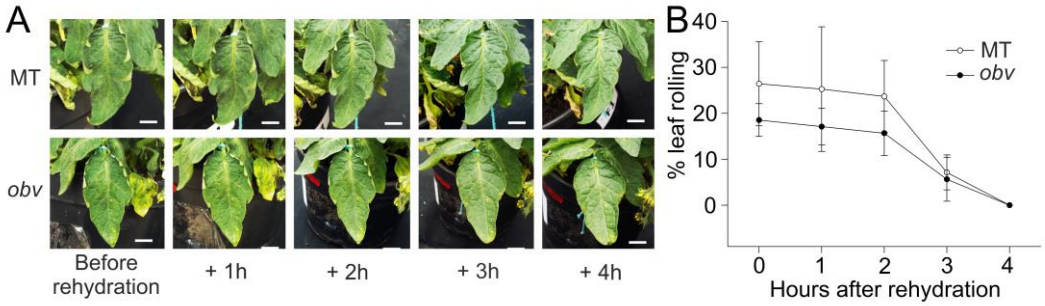

Figure S1. Phenotypes leaflets of tomato plants (cv. Micro-Tom) and *obv* mutant before and after rehydration (A). Figures are representative for MT plants and *obv* mutant. Images were obtained every hour after rehydration, for 4 consecutive hours. Leaf rolling rate evaluated for four hours, after hehydration (B). Measurements were performed of the central leaflet of the 5th fully expanded leaf. Bars represent the mean standard error of 6 repetitions Scale bars= 1 cm.

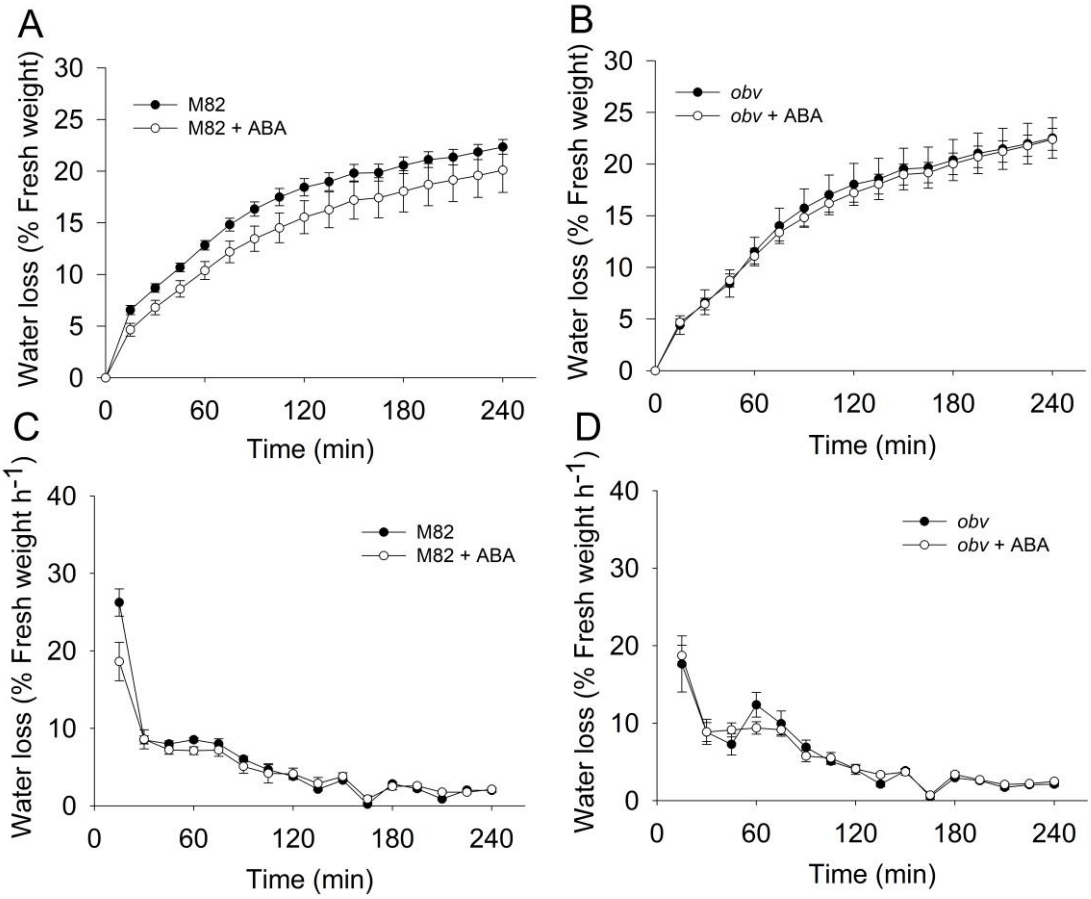

Figure S2. ABA reduces the water loss of M82 plants and does not reduce *obv* mutant. Leaves at the same developmental stage and size from 50 DAG plants were floated in MES-KCL buffer under light to induced stomatal apertures (control). Afterwards, leaves were incubated in ABA (50 µM) for 2.5h. The water loss of detached leaves was measured by weighing fresh leaves placed under a direct light source on the laboratory bench. Water loss was expressed as the percentage of initial weight at each time point. Data are averages of five repetitions for each treatment.

Literature cited

Araújo WL, Fernie AR, Nunes-Nesi A (2011) Control of stomatal aperture. Plant Signal Behav **6**: 1305–1311

Armacost R (1944) The structure and function of the border parenchyma and vein-ribs of certain dicotyledon leaves. Proc Iowa Acad Sci **51**: 157–169

Barradas VL, Jones HG (1996) Responses of CO_2 assimilation to changes in irradiance: laboratory and field data and a model for beans (*Phaseolus vulgaris* L.). J Exp Bot **47**: 639–645

Barrios-Masias FH, Chetelat RT, Grulke NE, Jackson LE (2014) Use of introgression lines to determine the ecophysiological basis for changes in water use efficiency and yield in California processing tomatoes. Funct Plant Biol **41**: 119–132

Berger D, Altmann T (2000) A subtilisin-like serine protease involved in the regulation of stomatal density and distribution in *Arabidopsis thaliana*. Genes Dev **14**: 1119–31

Blackman PG, Davies WJ (1983) The effects of cytokinins and aba on stomatal behavior of maize and commelina. J Exp Bot **34**: 1619–1626

Bolaños J, Edmeades GO, Martinez L (1993) Eight cycles of selection for drought tolerance in lowland tropical maize. III. Responses in drought-adaptive physiological and morphological traits. F Crop Res **31**: 269–286

Buckley TN (2005) The control of stomata by water balance. New Phytol **168**: 275–292

Buckley TN, Sack L, Farquhar GD (2016) Optimal plant water economy. Plant Cell Environ **40:** 1–16

Buckley TN, Sack L, Gilbert ME (2011) The role of bundle sheath extensions and

life form in Ssomatal responses to leaf water status. Plant Physiol. **156**: 962–973

Campos ML, Carvalho RF, Benedito VA, Peres LEP (2010) Small and remarkable. The Micro-Tom model system as a tool to discover novel hormonal functions and interactions. Plant Signal Behav **5**: 1–4

Carvalho RF, Campos ML, Pino LE, Crestana SL, Zsögön A, Lima JE, Benedito VA, Peres LE (2011) Convergence of developmental mutants into a single tomato model system: "Micro-Tom" as an effective toolkit for plant development research. Plant Methods **7**: 1-18

Chaumont F, Tyerman SD (2014) Aquaporins: Highly regulated channels controlling plant water relations. Plant Physiol. **164**: 1600-1618

Chitwood DH, Kumar R, Headland LR, Ranjan A, Covington MF, Ichihashi Y, Fulop D, Jiménez-Gómez JM, Peng J, Maloof JN, e outros (2013) A quantitative genetic basis for leaf morphology in a set of precisely defined tomato introgression lines. Plant Cell **25**: 2465–81

Cowan IR (1972) Oscillations in stomatal conductance and plant functioning associated with stomatal conductance: Observations and a model. Planta **106**: 185–219

Darwin F (1898) Observations on stomata. Philos Trans R Soc B Biol Sci **190**: 531–621

Eshed Y, Zamir D (1994) A genomic library of *Lycopersicon pennellii* in *Lycopersicon-esculentum* - a tool for fine mapping of genes. Euphytica **79**: 175–179

Farquhar GD, Ehleringer JR, Hubick KT (1989) Carbon isotope discrimination and photosynthesis. Annu Rev Plant Physiol Plant Mol Biol **40**: 503–537

Farquhar GD, Richards RA (1984) Isotopic composition of plant carbon correlates with water-use efficiency of wheat genotypes. Aust J Plant Physiol **11**:

539–552

Franks PJ (2001) The effect of exogenous abscisic acid on stomatal development, stomatal mechanics, and leaf gas exchange in *Tradescantia virginiana*. Plant Physiol **125**: 935–942

Hacker J, Neuner G (2007) Ice propagation in plants visualized at the tissue level by infrared differential thermal analysis (IDTA). Tree Physiol **27**: 1661–1670

Jones CM, Rick CM, Adams D, Jernstedt J, Chetelat RT (2007) Genealogy and fine mapping of Obscuravenosa, a gene affecting the distribution of chloroplasts in leaf veins and evidence of selection during breeding of tomatoes (*Lycopersicon esculentum*; Solanaceae). Am J Bot **94**: 935–947

Kadioglu A, Terzi R (2007) A dehydration avoidance mechanism: leaf rolling. Bot Rev **73**: 290–302

Kadioglu A, Terzi R, Saruhan N, Saglam A (2012) Current advances in the investigation of leaf rolling caused by biotic and abiotic stress factors. Plant Sci **182**: 42–8

Kagan ML, Novoplansky N, Sachs T (1992) Variable cell lineages form the functional pea epidermis. Ann Bot **69**: 303–312

Karabourniotis G, Bornman JF, Nikolopoulos D (2000) A possible optical role of the bundle sheath extensions of the heterobaric leaves of *Vitis vinifera* and *Quercus coccifera*. Plant, Cell Environ **23**: 423–430

Kawai K, Miyoshi R, Okada N (2017) Bundle sheath extensions are linked to water relations but not to mechanical and structural properties of leaves. Trees 1–11

Kenzo T, Ichie T, Watanabe Y, Hiromi T (2007) Ecological distribution of homobaric and heterobaric leaves in tree species of Malaysian lowland tropical rainforest. Am J Bot **94**: 764–775

Kim T-H, Bohmer M, Hu H, Nishimura N, Schroeder JI (2010) Guard cells signal transduction network: advances in understanding abscisic acid CO_2, and Ca^{2+} signalling. Annu Rev Plant Biol **61**: 561–591

Kirschbaum MUF, Gross LJ, Pearcy RW (1988) Observed and modelled stomatal responses to dynamic light environments in the shade plant *Alocasia macrorrhiza*. Plant, Cell Environ **11**: 111–121

Lawson T, von Caemmerer S, Baroli I (2010) Photosynthesis and stomatal behaviour. Springer Berlin Heidelberg, **72**: 265–304

Lawson T, Morison J (2006) Visualising patterns of CO_2 diffusion in leaves. New Phytol **169**: 641–643

Leegood RC (2008) Roles of the bundle sheath cells in leaves of C3 plants. J Exp Bot **59**: 1663–1673

Lind C, Dreyer I, López-Sanjurjo EJ, von Meyer K, Ishizaki K, Kohchi T, Lang D, Zhao Y, Kreuzer I, Al-Rasheid KAS, e outros (2015) Stomatal guard cells co-opted an ancient ABA-dependent desiccation survival system to regulate stomatal closure. Curr Biol **25**: 928–935

Lynch DJ, McInerney FA, Kouwenberg LLR, Gonzalez-Meler MA (2012) Plasticity in bundle sheath extensions of heterobaric leaves. Am J Bot **99**: 1197–1206

Maurel C, Verdoucq L, Rodrigues O (2016) Aquaporins and plant transpiration. Plant Cell Environ **39**: 2580–2587

McClendon JH (1992) Photographic survey of the occurrence of bundle-sheath extensions in deciduous dicots. Plant Physiol **99**: 1677–1679

Neger F (1918) Wegsamkeit der Laubblätter für Gase. Flora **111**: 152–161

Nicotra AB, Leigh A, Boyce CK, Jones CS, Niklas KJ, Royer DL, Tsukaya H

(2011) The evolution and functional significance of leaf shape in the angiosperms. Funct Plant Biol **38**: 535–552

Niklas KJ (2016) Plant Evolution, 1st ed. University of Chicago Press, Chicago, USA

Nikolopoulos D, Liakopoulos G, Drossopoulos I, Karabourniotis G (2002) The relationship between anatomy and photosynthetic performance of heterobaric leaves. Plant Physiol **129:** 235-243

Pacific Northwest Extension Group (2011) Physiological leaf roll of tomato. PNW616

Pieruschka R, Schurr U, Jensen M, Wolff WF, Jahnke S (2006) Lateral diffusion of CO_2 from shaded to illuminated leaf parts affects photosynthesis inside homobaric leaves. New Phytol **169**: 779–788

Powles JE, Buckley TN, Nicotra AB, Farquhar GD (2006) Dynamics of stomatal water relations following leaf excision. Plant, Cell Environ **29**: 981–992

Read J, Stokes A (2006) Plant biomechanics in an ecological context. Am J Bot **93**: 1546–1565

Roelfsema MRG, Hanstein S, Felle HH, Hedrich R (2002) CO_2 provides an intermediate link in the red light response of guard cells. Plant J **32**: 65–75

Ruszala EM, Beerling DJ, Franks PJ, Chater C, Casson SA, Gray JE, Hetherington AM (2011) Land plants acquired active stomatal control early in their evolutionary history. Curr Biol **21**: 1030–1035

Sack L, Holbrook NM (2006) Leaf hydraulics. Annu Rev Plant Biol **57**: 361–381

Sack L, Scoffoni C (2013) Leaf venation: structure, function, development, evolution, ecology and applications in the past, present and future. New Phytol **198**: 983–1000

Shimazaki K, Doi M, Assmann SM, Kinoshita T (2007) Light regulation of stomatal movement. Annu Rev Plant Biol **58**: 219–247

Sommerville KE, Sack L, Ball MC (2012) Hydraulic conductance of *Acacia phyllodes* (foliage) is driven by primary nerve (vein) conductance and density. Plant, Cell Environ **35**: 158–168

Terashima I (1992) Anatomy of nonuniform leaf photosynthesis. Photosynth Res **31**: 195–212

Von Caemmerer S, Lawson T, Oxborough K, Baker NR, Andrews TJ, Raines CA (2004) Stomatal conductance does not correlate with photosynthetic capacity in transgenic tobacco with reduced amounts of Rubisco. J Exp Bot **55**: 1157–1166

Von Groll U, Berger D, Altmann T (2002) The subtilisin-like serine protease SDD1 mediates cell-to-cell signaling during Arabidopsis stomatal development. Plant Cell **14**: 1527–39

Woltz S (1968) Influence of light intensity and photosynthate export from leaves on physiological leaf roll in tomatoes. Proc. Florida State Hortic. Soc. **81**: 208-211

Wylie RB (1952) The bundle sheath extension in leaves of dicotyledons. Am J Bot **39**: 645–651

Xu X, Martin B, Comstock JP, Vision TJ, Tauer CG, Zhao B, Pausch RC, Knapp S (2008) Fine mapping a QTL for carbon isotope composition in tomato. Theor Appl Genet **117**: 221–233

Zeiger E, Iino M, Ogawa T (1985) The blue light response of stomata: pulse kinetics and some mechanistic implications. Photochem Photobiol **42**: 759–763

Zsögön A, Alves Negrini AC, Peres LEP, Nguyen HT, Ball MC (2015) A mutation that eliminates bundle sheath extensions reduces leaf hydraulic conductance, stomatal conductance and assimilation rates in tomato (*Solanum*

lycopersicum). New Phytol **205**: 618–626

Zwieniecki MA, Brodribb TJ, Holbrook NM (2007) Hydraulic design of leaves : insights from rehydration kinetics. Plant, Cell Environ **30:** 910–921

GENERAL CONCLUSIONS

Considering the information produced in this work, we bring here our considerations about the relation of BSE to the structural and physiological characteristics of the leaves in the face of environmental changes. Our results demonstrate that, BSE coordinated structural and physiological changes in tomato leaves at different levels of irradiance. Heterobaric leaves showed phenotypic plasticity, mainly in relation to vein density and SPI, showing that BSE acts by coordinating the flow of water from the vascular bundle to the epidermis, when the levels of irradiance are low. The structural and physiological changes observed in homobaric plants at different levels of irradiance, such as an increase in intercellular air spaces, suggest that the absence of BSE contributed to maintain the diffusion of CO_2 in the intercellular spaces in the shade condition. Here we also show other relevant information about BSE, whose absence may be associated with better plant performance when a soil drought occurs. Studies have shown that BSE has played roles in the water relations of plants, but these responses may differ between species. Our results revealed that, the presence of BSE, promoted direct effects with the responses of these plants in dry conditions. Kawai et al. (2017) proposed that BSE would be associated with plant water relations, and found positive correlations between higher BSE density (D_{BSE}) and g_s values at noon, and in contrast, negative correlations between higher D_{BSE} and Ψl_{eaf}, indicating that heterobaric leaves are more prone to water loss. Considering this information, we consider that homobaric leaves respond better to the water deficit because they present lower vein density and, therefore, present a slower distribution of water (K_{leaf}), maintaining leaves with greater hydration for longer. In fact, this work has provided evidence that BSE has a strong influence on the plasticity of the leaves at different levels of irradiance and also influences the water relations. *obv* mutant, which have homobaric leaves, showed greater resistance to the effects of lack of water in the soil, in visual and hydration terms, and developed modulations in leaf structures to ensure the maintenance of physiological mechanisms in low irradiance. Thus, our results

demonstrated that, structural characteristics of leaves, have a direct effect on the physiological responses of plants to environmental changes. However, we propose that further evaluations should be carried out in order to better clarify the possible relations that BSE may have with the stress responses of plants such as those presented here, among others.